HYDROGEN EMBRITTLEMENT OF IRON ALUMINIDES

by
ARVIND AGARWAL

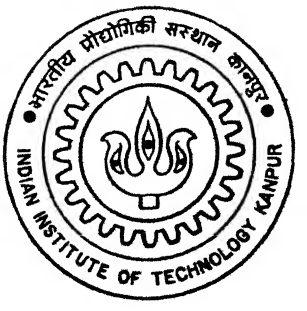

DEPARTMENT OF MATERIALS AND METALLURGICAL ENGINEERING
INDIAN INSTITUTE OF TECHNOLOGY KANPUR
JANUARY, 1995

HYDROGEN EMBRITTLEMENT OF IRON ALUMINIDES

A Thesis Submitted

in Partial Fulfillment of the Requirement

for the Degree of

MASTER OF TECHNOLOGY

by

ARVIND AGARWAL

to the

DEPARTMENT OF MATERIALS AND METALLURGICAL ENGINEERING

INDIAN INSTITUTE OF TECHNOLOGY KANPUR

JANUARY 1995

MME – 1995 – M – AGA – HYD

TO

MY ALTER EGO, MANISH

CERTIFICATE

It is certified that the work contained in the thesis entitled "*Hydrogen Embrittlement of Iron Aluminides*", by Arvind Agarwal, has been carried out under my supervision and that this work has not been submitted elsewhere for a degree.

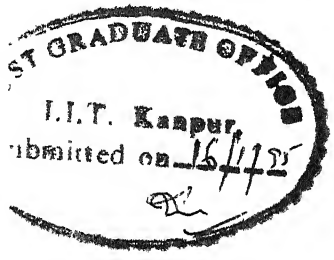

Dr. R. Balasubramaniam
Assistant Professor
Department of Materials and Metallurgical Engineering
Indian Institute of Technology Kanpur

January 1995

ACKNOWLEDGEMENT

I take the opportunity to express my heartfelt gratitude to my thesis supervisor Dr. R. Balasubramaniam whose able guidance was always the source of inspirations during the project work.

I also thank Dr. S. Bhargava for his valuable suggestions in the initiation of this study.

I express my gratitude to my friends K.S. Rao, Satyam, Sujata, Shailesh, Akhtar, Vidya, Thakurji, Rupa and Kameshwar for reaching out their hands at crucial time.

A special thank is owed to Dr. M.N. Mungole, for his continuous support throughout the study of this work. I thank Mr. V P. Gupta for his technical expertise while using arc furnace.

I am extremely thankful to DMRL, Hyderabad for providing the material for this study.

Arvind Agarwal

TABLE OF CONTENTS

ABSTRACT

The room temperature hydrogen embrittlement problem in iron aluminides has restricted their use as high temperature structural materials. The role of thermomechanical and heat treatments in affecting the mechanical properties has been studied from a processing-structure-properties correlation view point. Alloying additions to iron aluminides have been done to improve their ductility.

It has been found that intermetallic rolled at higher temperature exhibited higher fracture strength. This has been attributed to fine subgrain size (28μ) due to dynamic recrystallisation occurring at higher rolling temperature of 1000^{o}C. However, intermetallic rolled at 1000^{o}C and then recrystallised showed highest ductility but poor fracture strength. This behaviour has been ascribed to the partially recrystallised microstructure. Partially recrystallised microstructure prevents hydrogen ingress through grain boundaries and minimises hydrogen embrittlement. The intermetallic rolled at 1000^{o}C and then ordered at 500^{o}C for 100 hours showed highest fracture strength due to its finer grain size. The intermetallic rolled at 500^{o}C and then ordered had undergone grain growth. Hence, they exhibited lower fracture strength of 360 MPa. Fracture morphologies were brittle and exhibited cleavage type fracture in all the cases.

Fe_3Al-5Ta, Fe_3Al-5Nb, Fe_3Al-5Mo, Fe_3Al-5Si and Fe_3Al-5V cracked during rolling. This suggested formation of the brittle phase(s). However, Fe_3Al-5Cr and Fe_3Al-5Ti could be rolled to 80% deformation successfully without cracking. Chromium and titanium additions to iron aluminides have provided improved ductility. The formation of surface passive layer is envisaged to the improvement in ductility in these intermetallics.

LIST OF FIGURES

LIST OF TABLES

CHAPTER 1

INTRODUCTION

Ordered iron aluminide intermetallics of composition Fe_3Al and FeAl possess attractive properties for application as structural materials at elevated temperature in aggressive environments. However, their poor room temperature ductility limits their use as engineering materials as they are difficult to process into useful shapes like plates and tubes. In recent years, efforts have been intensified to identify both the extrinsic and intrinsic factors governing room temperature brittle fracture.

Several studies have established that the poor room temperature ductility is caused mainly by an extrinsic effect - environmental embrittlement due to hydrogen.

Several methods have been proposed to minimize hydrogen embrittlement (HE) in iron aluminides. Most of the methods that have been suggested to curb HE aim to restrict entry of hydrogen into the lattice by providing a passive film on the iron aluminide surface. Oxide coatings have been beneficial in increasing the ductility of iron aluminides. Another method for improving the ductility of iron aluminides is by the addition of chromium. Even small chromium additions are effective in minimizing hydrogen embrittlement and in providing increased ductility. However, the role of chromium in affecting hydrogen embrittlement and in causing ductility enhancements is still unresolved.

Thermomechanical treatments (TMT) also play a very crucial role in improving the mechanical properties of iron aluminides.

The present investigation aims at the development of novel ductile iron aluminide intermetallics with the help of thermomechanical treatments and alloying with those elements which would enhance the passive surface layer. Chapter 2 deals with the review of the literature. Experimental procedures are discussed in Chapter 3. Chapter 4 presents the results and discussion of this study while Chapter 5 incorporates conclusions and suggestions for further study.

CHAPTER 2

LITERATURE REVIEW

Ordered intermetallics constitute an unique class of metallic materials that form long-range-ordered crystal structures below a critical temperature that is generally referred to as the critical ordering temperature (Tc) [1]. These intermetallics usually exist in relatively narrow compositional ranges around simple stoichiometric ratios. The search for new high-temperature structural materials has stimulated much interest in ordered intermetallics. Intermetallic aluminides possess many attributes that make them attractive for high temperature structural applications [2]. They contain enough aluminium to form, in oxidizing environments, thin films of aluminium oxides that are often compact and protective. They have low densities, relatively high melting points and good high strength properties.

2.1 IRON ALUMINIDES

Ordered iron aluminides exist in relatively narrow compositional ranges around simple stoichiometric ratios (Figure 1). Iron aluminides based on Fe_3Al and FeAl can exist in two crystal allotropic modifications. These structures (DO_3 and B2) are both ordered BCC structures and these are presented in Figure 2. Fe_3Al can exist both as B2 and DO_3 ordered structure (depending upon the temperature, Figure 1) while FeAl can exist only in the B2 ordered form [3]. Table 1 presents some typical room temperature properties and critical ordering temperatures for

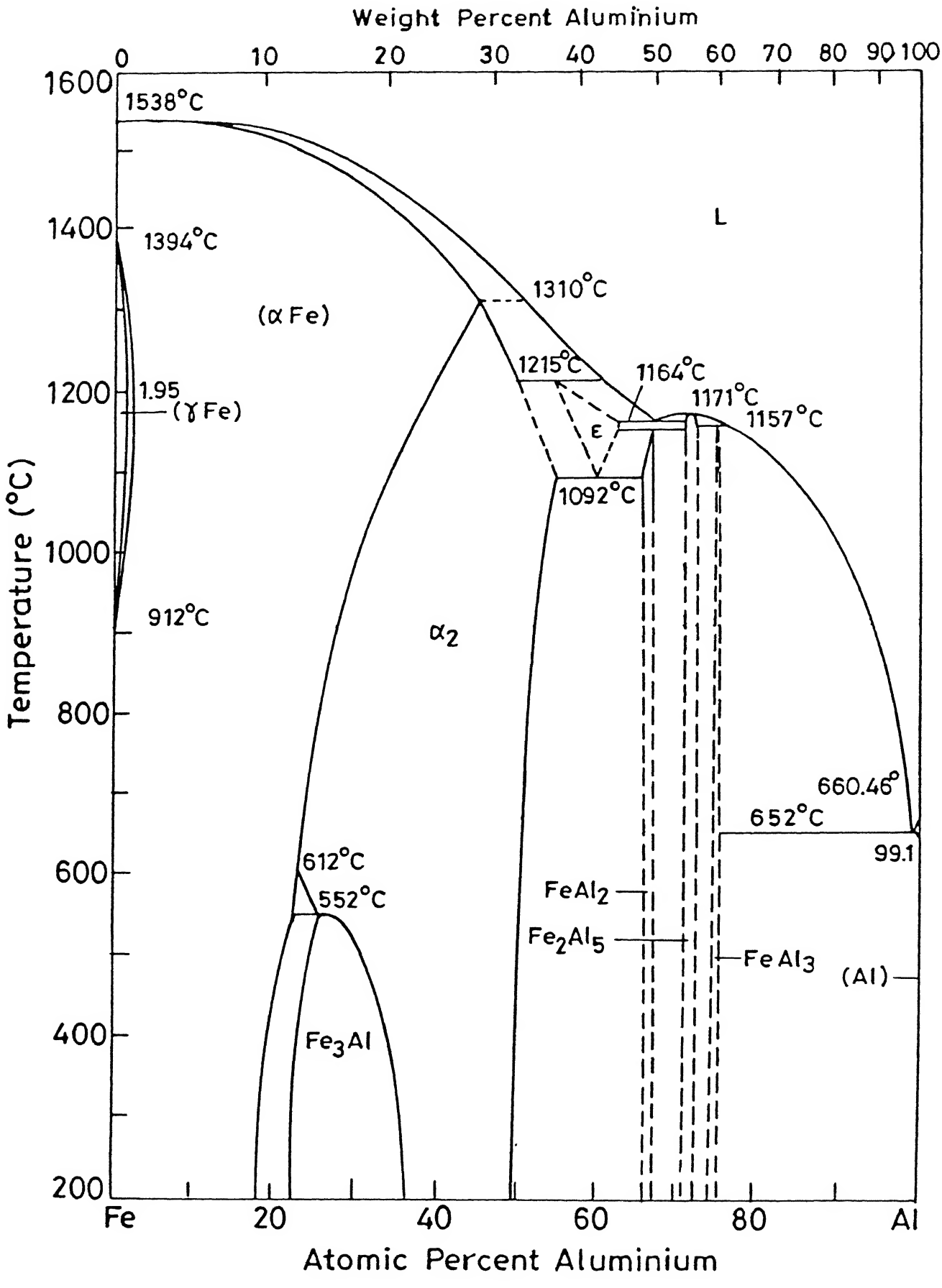

Fig. 1. The Fe-Al phase diagram.

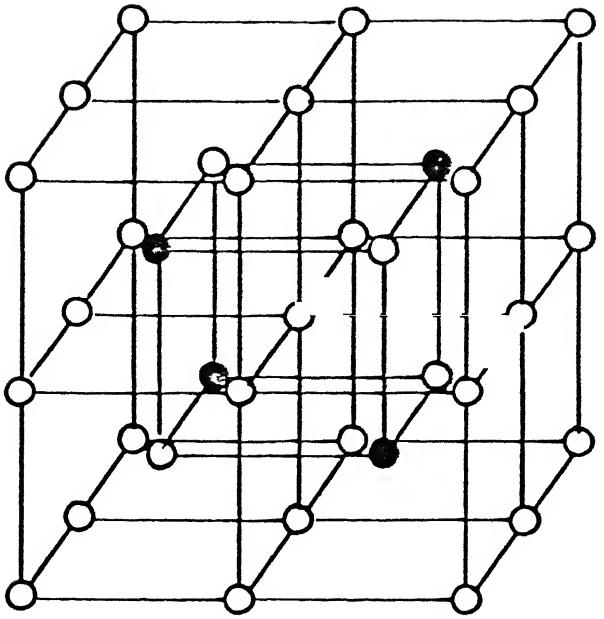

$Fe_3Al\ (DO_3)$

○ Fe ● Al

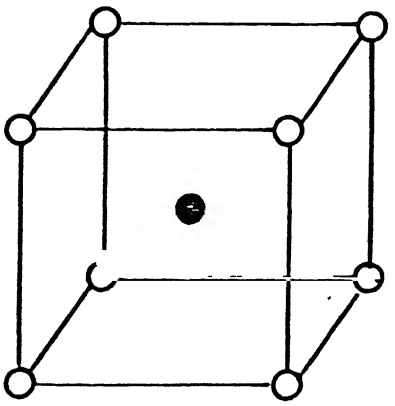

FeAl (B2)

Fig. 2. The DO_3 and B2 ordered crystal structures of iron aluminides.

Table 1 Typical Room Temperature Properties of Iron Aluminides

Alloy	Crystal Structure	Temp. (^{o}C)		Density (gm/cc)	Room Temp. Y.Strength (MPa)	Room Temp. Elongation (%)
		order -ing	M.P.			
Fe_3Al	DO_3	540	1540	6.72	300	3.7
Fe_3Al	B2	760	1540	6.72	380	4.1
FeAl	B2	1250	1250	5.56	360	2.2

different allotropic modifications of iron aluminides [3].

Iron aluminides have excellent oxidation and corrosion resistance because they are capable of forming protective oxides scales as elevated temperature in hostile environments [4]. Iron aluminides exhibit corrosion or oxidation rates lower than those of promising iron-based alloys by a couple of orders of magnitude even in a severe sulphidizing environment (Figure 3) [5].

Some other advantages of iron aluminides are:

i) Low material cost

ii) Relatively low density and

iii) Conservation of strategic material such as chromium.

However, the major drawbacks of these aluminides are poor ductility and brittle fracture at ambient temperatures and poor strength and creep resistance above 600°C.

2.2 HYDROGEN EMBRITTLEMENT OF IRON ALUMINIDES

Iron aluminides have been known to be brittle at room temperature for more than 50 years since the first study conducted in 1930 [6]. However, the major cause of their low ductility and brittle fracture was not known until recently [7]. Shan and Lin have studied the effect of strain rate on ductility of iron aluminides[8]. They have confirmed that ductility of Fe_3Al alloys is sensitive to strain rate. This indicates that some time dependent phenomenon is occurring in these alloys. It is well known that when the specimen is under tension in air, the following reaction occur at the metal surface [8]

$$3H_2O + 2Al = Al_2O_3 + 6H$$

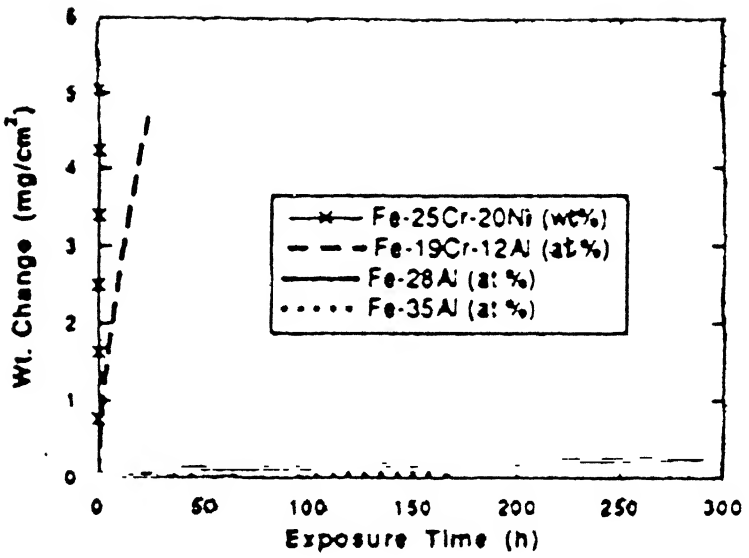

Fig.3 Weight gain curves for Fe based alloys in sulfidizing environment at high temperature.

This atomic hydrogen penetrates into the metal and causes crack propagation. At very low strain rates, atomic hydrogen gets enough time to diffuse in and accumulate at crack tips, which results in brittle fracture. At high strain rates, atomic hydrogen does not get enough time to diffuse and cluster and so iron aluminides show higher ductility. The effect of strain rate on ductility in air and in vacuum has been studied by Kasul and Heldt on Fe-35Al alloy [9] (Figure 4).

Figure 4 clearly indicates that elongation measured in air is sensitive to strain rate while elongation measured in vacuum is independent of strain rate. The strain rate dependence behaviour of Fe-35Al is very similar to that of Fe-28Al, as measured by Shan and Lin [8]. The effect of strain rate on the ductility of Fe_3Al in air clearly proves that the embrittlement is due to hydrogen.

That hydrogen is the main damaging agent causing poor ductility can also be inferred from tensile tests conducted in different environments. These results are summarized in Table 2 [10].

The effect of various test environments on the room temperature stress-strain behaviour of iron aluminides is shown schematically in Figure 5.

As evident from Figure 5, ductility is higher in Ar + 4% H_2 environment rather than humid air. This is because molecular hydrogen does not cause much embrittlement in Fe_3Al, because of its lower activity as compared with atomic hydrogen produced from water vapor reaction. As seen in this figure, testing in water vapour environment show the least ductility and vacuum/oxygen

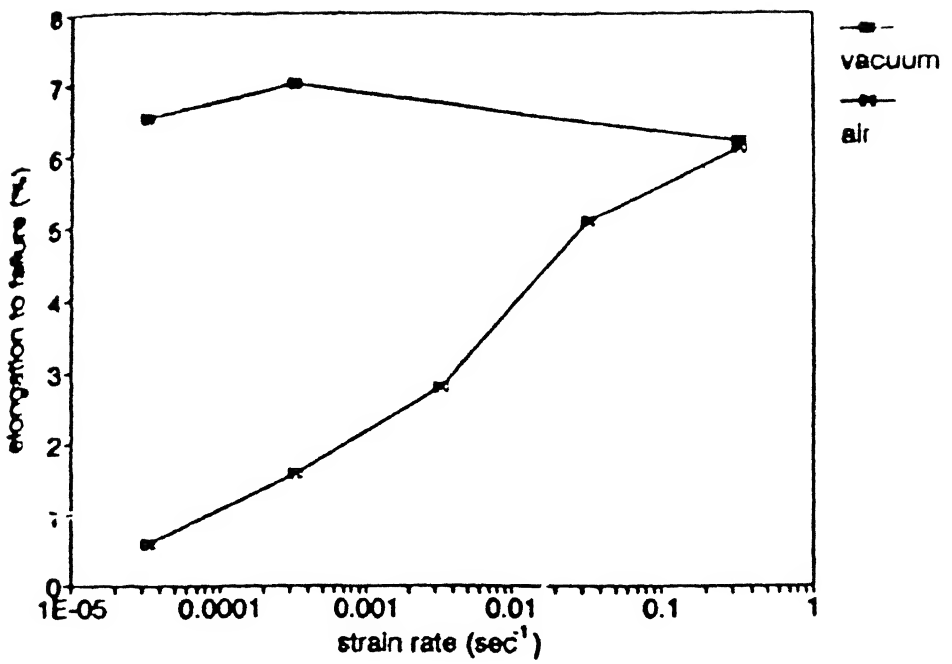

Fig.4 Effect of strain rate on the ductility of Fe-35Al allo

Table 2 Room Temperature Tensile Properties of Fe_3Al in Different Test Environments.

Environment	Yield Strength (MPa)	UTS (MPa)	Ductility (%)
	Heat Treated for 2 hr at 700°C (B2 Structure)		
Vacuum	387	851	12.8
Oxygen	392	867	12.0
Ar + 4% H_2	385	371	8.4
Air	387	559	4.1
H_2O vapour	387	475	2.1
	Heat Treated for 120 hr at 500°C(DO_3 Structure)		
Vacuum	316	813	12.4
Oxygen	298	888	11.7
Air	279	514	3.7
H_2O vapour	322	439	2.1

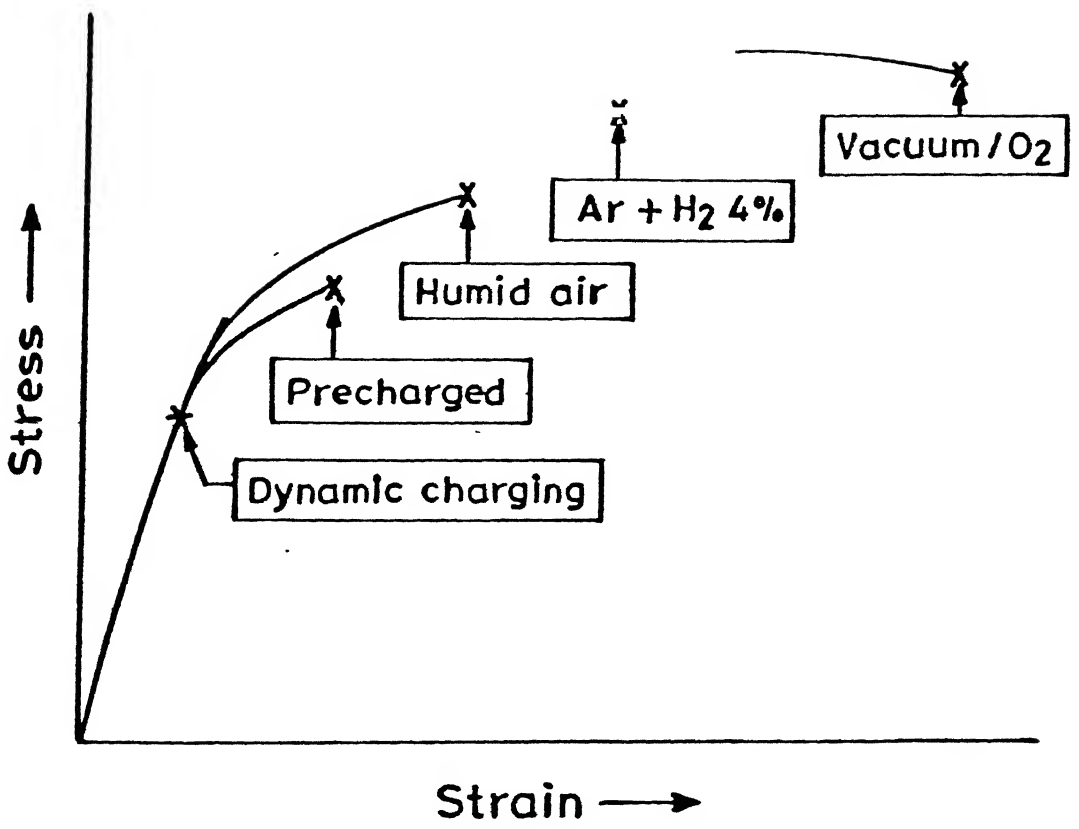

Fig.5 Schematic tensile stress-strain behaviour of iron aluminides in various environments at ambient temperature.

environments provide high ductility. Liu et al. have shown that higher ductilities are observed in a dry oxygen environment rather than in vacuum because oxygen reacts with aluminium to form Al_2O_3 directly [10]

$$2Al + \frac{3}{2} O_2 = Al_2O_3 \qquad (1)$$

and thereby suppressing the aluminium-moisture reaction which provides nascent hydrogen.

$$2Al + 3H_2O = Al_2O_3 + 6H \qquad (2)$$

Generation of atomic hydrogen is suppressed and thus higher ductility is observed in dry oxygen environment.

There is no unique mechanism which has been universally accepted to explain hydrogen embrittlement of iron aluminides. However, the process of HE is iron aluminides can be visualized as follows. The reaction that provides nascent hydrogen which embrittles iron aluminides is (2) above. The propensity of the above reaction increases with increasing aluminium concentration in iron aluminides [10]. The reaction of condensed moisture from ambient environments with aluminium at crack tips and freshly created metal surfaces (due to oxide spallation) results in the generation of high fugacity atomic hydrogen that causes severe embrittlement. This process is schematically illustrated in Figure 6.

Kasul et al. studied the effect of hydrogen precharging into iron aluminide on its mechanical properties [11]. Precharged specimens were tested in vacuum. They showed similar results to specimen tested in air. Ductility was severely reduced in both the cases. This proves that source of embrittlement must be

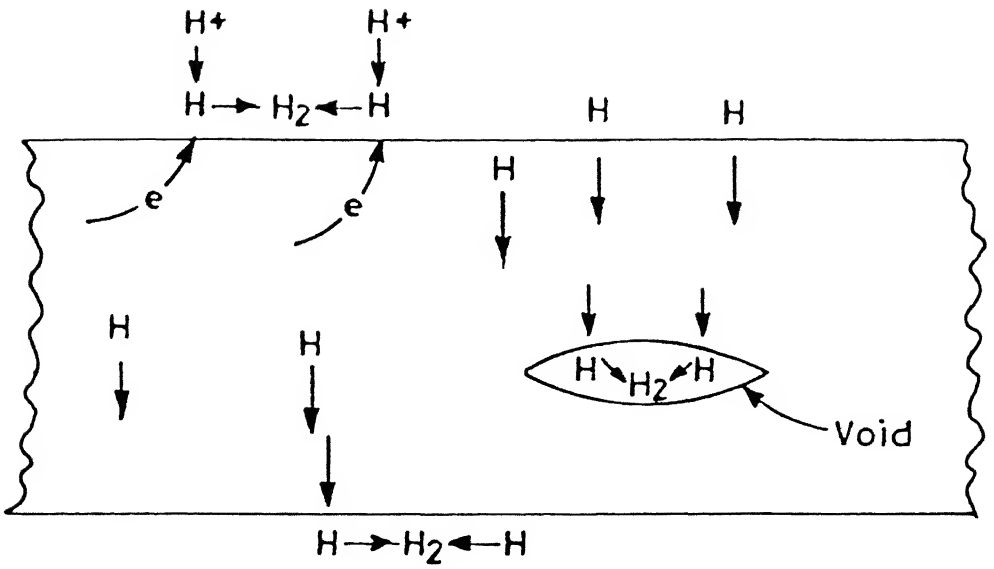

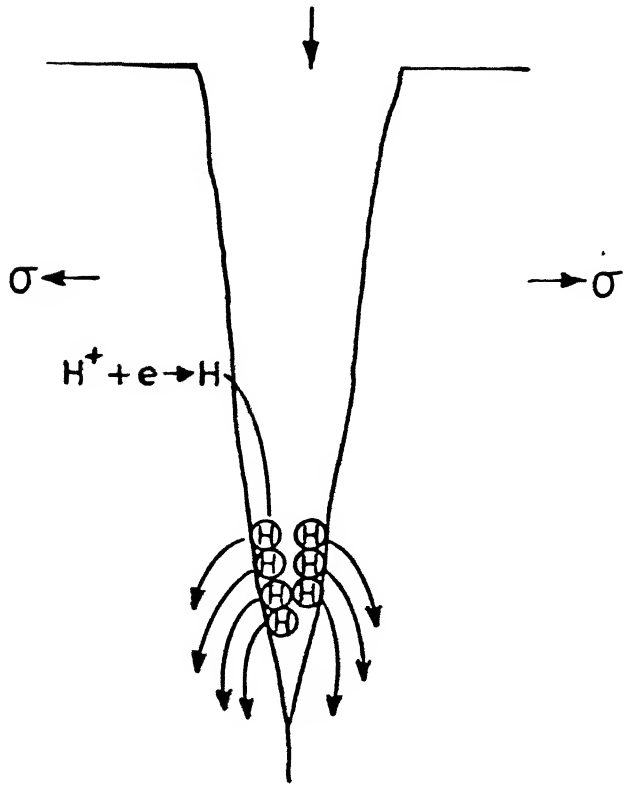

Fig.6 Hydrogen entry into the material and processes that occur at the crack tip during hydrogen embrittlement.

internal to the specimen, as there is presumably no external embrittling agent in the vacuum. Thus, it was concluded that internal atomic hydrogen was responsible for embrittlement in precharged iron aluminide specimens. Kasul et al. also performed in-situ testing in aqueous solution by polarizing the material cathodically in Na_2SO_4 solution so that hydrogen is formed at the specimen surface during straining [11]. The ductility was reduced sharply in this case. However, anodic polarization did not show any drop in ductility (with reference to air). A similar result was also obtained for NaOH solution (Figure 7) [11].

These results indicate that when there is a high fugacity of hydrogen at the specimen surface, the ductility is low. This result is also reflected in Figure 5 which shows that dynamic hydrogen charging gives least ductility in iron aluminides.

2.2.1 Effect of Hydrogen Content

Kasul and Heldt have elucidated the effect of hydrogen content in iron aluminides on its mechanical properties [9]. Figure 8 shows the hydrogen content of Fe-35Al samples cathodically charged for different lengths of time. It is seen that increasing charging time results in decreasing ductility. Figure 9 shows the effect of cathodic charging time on the ductility of Fe-35Al tested in vacuum. This result further confirms that embrittlement increases with an increase in hydrogen content. However, ductility can be restored in these cathodically charged iron aluminides by following a suitable baking schedule. Table 3 shows the baking schedule followed by Kasul and Heldt [11].

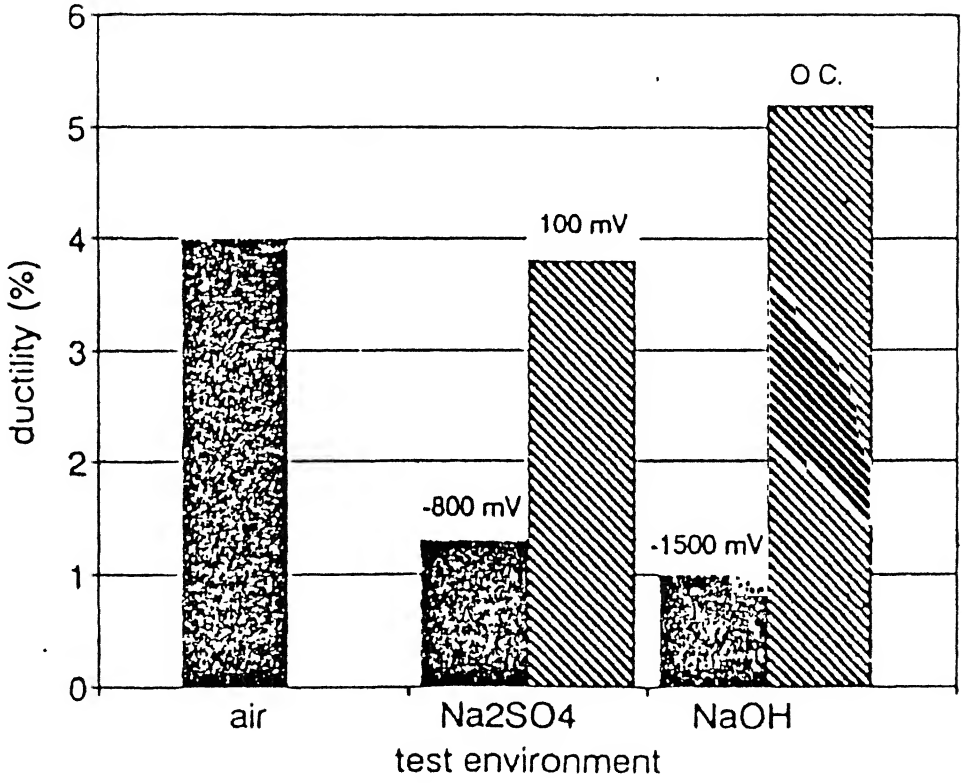

Fig.7 Ductility of Fe-24.6Al under conditions of controlled potential and pH (electrochemical potentials are with reference to SCE).

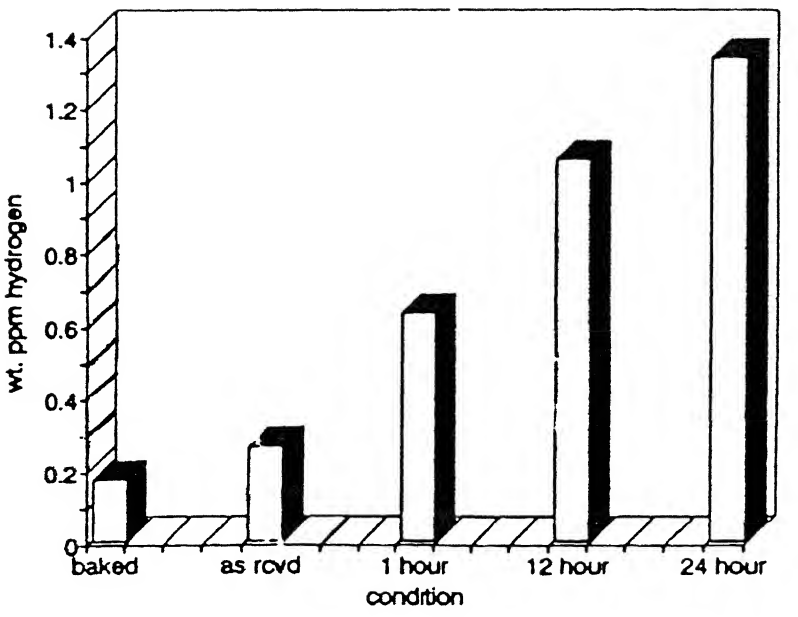

Fig.8 Hydrogen content analysis of Fe-35Al charged in 1N H_2SO_4

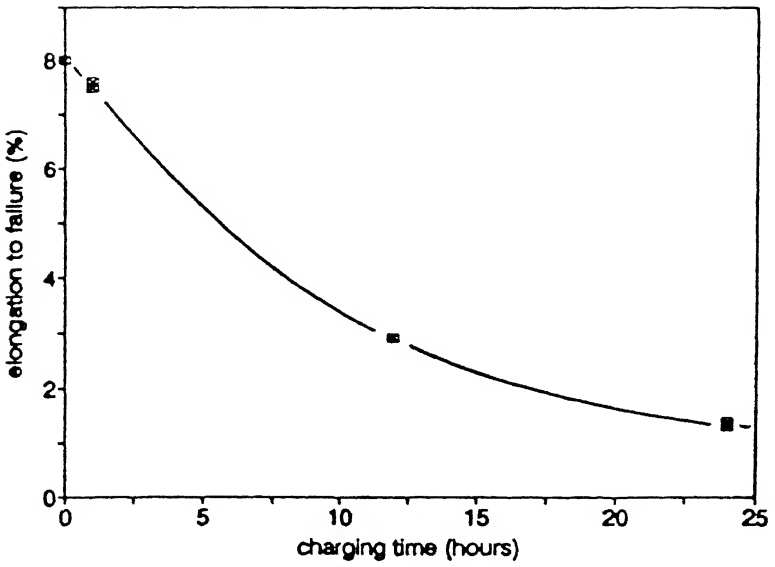

Fig.9 Effect of cathodic charging time on the ductility of Fe-35 Al tested in vacuum.

Table 3 Percentage of ductility restored after various baking treatments for specimens precharged 1 hour in sulfuric acid.

Bakeout Temp. (^{o}C)	Bakeout Time	Percentage of ductility restored
23 (vacuum)	75 days	0
200 (air)	24 hours	65
200 (air)	48 hours	90-100
800 (air/vac)	1 hour	100

Although ductility cannot be fully restored even after baking for very long times at room temperature in a vacuum, full ductility was restored by baking at 800°C for one hour. The full recovery of the ductility reflects that embrittlement is a reversible phenomenon in cathodically charged iron aluminides. Kasul and Heldt have used diffusion equations to simulate baking kinetics and thus have suggested the baking schedule for precharged iron aluminide samples to eliminate hydrogen [9].

2.3 MECHANISMS OF HYDROGEN EMBRITTLEMENT

There is yet no single mechanism which has been fully accepted in understanding the mechanism of hydrogen embrittlement in iron aluminides.

Birnbaum et al. have proposed a mechanism known as Hydrogen Enhanced Localized Plasticity (HELP) [12]. This mechanism suggests that hydrogen increases plasticity at the crack tip in many metals and alloys, leading to brittle fracture. There is a controversy about this mechanism that whether hydrogen influences plasticity through the volume or the surface. But there are enough evidences to prove slip localization due to hydrogen near a crack tip in several fcc and bcc metals [12].

Bond et al. have suggested another mechanism in which hydrogen facilitates dislocation motion [13]. This increased dislocation mobility throughout the lattice increases the crack growth rate and hence brittle fracture occurs.

Generally, the fracture appearance in this class of intermetallics is of the cleavage type, with facets of {100} type suggesting "decohesion" as the possible mechanism of hydrogen

embrittlement. The decohesion mechanism of hydrogen embrittlement is shown in Figure 10. Hydrogen enters the material after bulk diffusion or grain boundaries diffusion and adsorption on the surface. This hydrogen is supposed to lower the bond strength in iron aluminides [14].

Evidence for decohesion mechanism is based upon the brittle appearance of fracture surface and the propensity for cleavage on {001} planes in embrittled single crystals of intermetallic aluminides [15]. Moreover, the brittle appearance of hydrogen induced (or moisture induced) fatigue cracks in iron aluminides alloys also suggests decohesion as the likely mechanism of hydrogen embrittlement [15].

2.4 SURFACE PASSIVE LAYER EFFECT

It has been observed that ductility is higher in dry oxygen environment. It suggests that by promoting the formation of an oxide layer on the surface it should be possible to minimize hydrogen entry into the lattice and limit the subsequent hydrogen embrittlement phenomenon.

Of the several methods which have been adopted to minimize HE of iron aluminides, chromium additions have been very useful in increasing ductility by an order of magnitude [16]. Table 4 summarizes the tensile behaviour of iron aluminides where the effect of chromium addition can be observed[16]. The exact mechanism for the increase in ductility by Cr additions is yet unresolved. However, Mckamey and Liu suggested that the beneficial effect of Cr comes from surface oxide modification, rather than modification of bulk properties [17]. They suggested

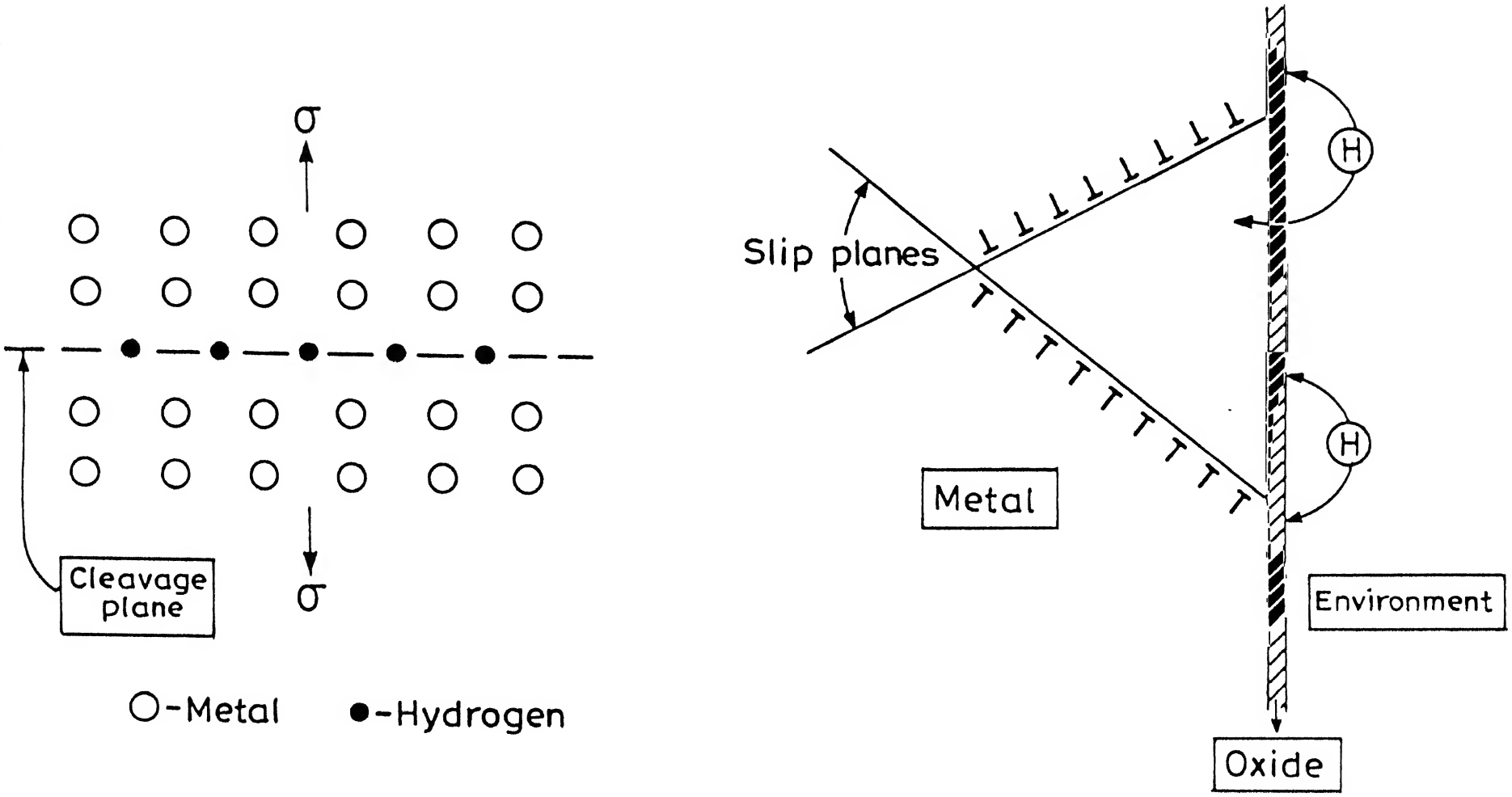

Fig.10 Hydrogen embrittlement mechanism by decohesion in iron aluminides.

Table 4 Room Temperature Mechanical Properties of Fe_3Al and Fe_3Al + Cr Alloys.

Alloy	Yield Strength (MPa)	UTS (MPa)	Ductility (%)
Fe-28Al	279.2	514.4	3.7
Fe-28Al-2Cr	247.2	638.5	9.4
Fe-28Al-4Cr	228.2	553.4	8.2
Fe-28Al-6Cr	232.4	535.4	8.4

a change in oxide chemistry and properties or a change in the kinetics of oxide formation, thereby reducing the water-vapor reaction. A mechanism for the chromium alloying effect has been recently proposed and it is based on reduction of hydrogen reduction reaction rates on passivated iron aluminide surfaces [14]. This mechanism suggests that the entry of hydrogen into the lattice can be checked and HE minimized.

The effect of surface modifications on the hydrogen embrittlement behaviour of iron aluminides can be seen in Table 5 [17]. The surface nature can be manipulated by several methods such as i) electropolishing, ii) oxide coating , and iii) alloying. The first two aspects were studied in detail by McKamey and Liu [17].

Tensile tests were carried out on iron aluminides having the following surface conditions:

a) Electropolished surface (produced by first grinding to remove as received oxide and then electropolishing),

b) As received (as rolled) condition consisting of a thin oxide film formed during rolling, and

c) Oxide coated (by oxidizing iron aluminide in air).

Table 5 summarizes the tensile behaviour of these specimens. It is obvious from Table 5 that ductility increases upon oxide coating. Several other inferences can also be drawn from Table 5 concerning Cr containing iron aluminides. The samples which were electropolished and then annealed in vacuum to minimize oxide reformation show ductility comparable to the binary Fe_3Al intermetallic in both the B2 and DO_3 ordered conditions. There is

Table 5 Effect of Surface Condition on Room Temperature Mechanical Properties of Fe_3Al and Fe_3Al + Cr Alloys.

Crystal Structure	Surface Condition	Fe_3Al(28 at% Al)			Fe_3Al-4Cr		
		Y.S (MPa)	UTS (MPa)	Elong. (%)	Y.S (MPa)	UTS (MPa)	Elong. (%)
B2	Elect.Polish	387	559	4.1	256	364	4.0
	As Rolled	398	587	4.3	199	433	7.8
DO_3	Elect.Polish	267	515	5.4	192	356	5.8
	As Rolled	277	551	5.6	196	423	7.2
DO_3	Oxide Coated	270	429	3.6	236	483	8.2
	As Rolled	285	466	3.6	248	461	7.0

a significant increase in ductility for Cr containing samples as compared to the base Fe_3Al intermetallic in the as rolled condition. Chromium containing specimens which were heat treated for 96 hours at 500°C in air (to give the DO_3 crystal structure) show comparable ductilities, whether they were oxide coated or present in the as rolled condition. Also, the ductility of the oxide coated (Cr containing) intermetallic is higher than the electropolished specimen. These results strongly suggest that surface passive films on iron aluminides restrict hydrogen embrittlement. It is interesting to note that corrosion characteristics can also be improved by surface conditioning.

2.5 EFFECT OF MICROSTRUCTURE

It is important to mention that recrystallisation processes vary greatly in Fe_3Al system with several variables such as thermo -mechanical treatments, alloying, crystal structure and microstructure [4]. Thus, it is very difficult to predict exactly about recrystallisation temperature and kinetics in Fe_3Al system.

McKamey and Pierce have studied the effect of annealing temperature on the mechanical behaviour of iron aluminide [18]. Table 6 shows the effect of different heat treatments on iron aluminides [18]. This effect has been further elucidated in Figure 11 [18]. It is clear that ductility improves after annealing treatment at 750°C for 1 hour. This treatment produces a stress relieved but partially recrystallised microstructure. Table 6 and Figure 11 reflect that increasing the degree of recrystallisation results in loss of ductility and tensile strength. A completely recrystallised microstructure produces

able 6 Effect of Recrystallization on Room Temperature Tensile Properties of a Fe_3Al Alloy[a]

Heat treatment[b] (h/°C)	Fraction recrystallized (%) (grain size, μm)	Yield stress (MPa)	Fracture stress (MPa)	Elongation (%)
1/550	0	550	760	5.4
1/650	0	543	807	8.1
1/750	10	479	736	8.0
1/850	20	453	670	6.4
1/1000	100 (41)	280	413	3.0
1/1100	100 (68)	279	450	4.0
0.5/750	<5	481	736	8.2
1/750	10	466	710	7.8
4/750	25	438	665	7.8
24/750	50 (20-30)	369	577	5.2
48/750	80 (20-60)	328	492	4.4
0.17/1000	100 (34)	288	439	3.6
0.5/1000	100 (36)	287	425	3.0
1/1000	100 (43)	274	436	3.2
4/1000	100 (45)	277	422	3.0

[a]Alloy composition, Fe-28Al-5Cr-0.1Zr-0.05B (at.%).
[b]All alloys were heat treated 1 h at 700°C before punching test specimens. After the recrystallization heat treatment, all specimens were annealed for 3 d at 500°C to establish DO_3 order.

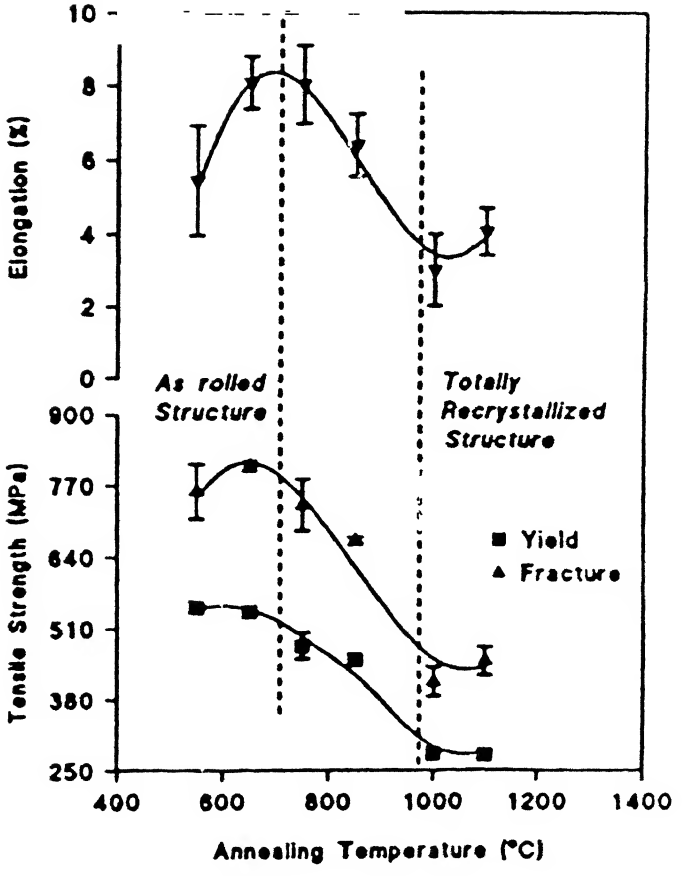

Fig.11 Effect of annealing temperature on room temperature properties of a Fe_3Al based alloys.

least desirable mechanical properties. These results indicate that a stress relieved and partially recrystallised microstructure minimizes environmental embrittlement in iron aluminides. The exact mechanism of minimizing embrittlement by controlling the microstructure is yet unresolved. One of the mechanism suggests that elongated grain structure characteristic of as rolled and partially recrystallised structures provides a minimum of transverse cleavage planes as well as a minimum of grain boundary area. This suppresses the atomic hydrogen ingress and also the grain boundary diffusion of hydrogen is reduced. Hence, HE is also minimized [18].

2.6 EFFECT OF ALLOYING ADDITIONS TO IRON ALUMINIDE

Alloying addition has been one of the schemes used to improve the ductility of iron aluminides. Alloying controls surface condition, reduction in hydrogen solubility and diffusion, refinement of grain structure, enhancement of grain boundary cohesion, grain shape and recrystallisation condition [3]. Effect of chromium addition to iron aluminides has been already reviewed in Section 2.4.

Boron addition (in ppm range) has been found to be very effective in increasing the grain boundary cohesiveness in ordered intermetallic alloys [19]. Boron has been also effective for Fe-Al class of aluminides. Boron segregates at grain boundaries and reduces intrinsic brittleness of B2 iron aluminide [20].

The strength of Fe_3Al and FeAl alloys at high temperatures is improved by alloying with elements such as Mo, Nb and Ti [21]. There is a positive change in the $DO_3 \longrightarrow B2$ transition

temperatures on alloying with Mo and Ti [21]. Large shift in the critical ordering temperature could prove to be very beneficial, as it will save energy by reducing the ordering time.

Zirconium has been alloyed to Fe_3Al to strengthen grain boundaries and to prevent recrystallisation. McKamey and Pierce have already confirmed that partially recrystallised microstructure reduces hydrogen embrittlement[18]. Thus, zirconium can help in preventing hydrogen embrittlement.

Recently, Lin et al. have studied the effect of Ti addition to Fe_3Al [22]. They have demonstrated superplasticity in the Fe_3Al-2Ti alloy at high temperature (Figure 12). Strain rate sensitivity 'm' value of 0.32 showed the highest elongation. Interestingly, this alloy showed superplastic behaviour even at a large grain size of 100 μm. This has been ascribed to the process of dynamic recovery and recrystallization occuring in Fe_3Al-2Ti intermetallic at high temperature.

Bordeau have explained the effect of second phase particles such as TiB_2 on ductility of Fe_3Al and FeAl [23]. TiB_2 helps in grain refinement during powder extrusion of Fe_3Al based alloys. However, TiB_2 addition has been found to be detrimental for weldability of iron aluminides, as it promotes hot cracking [24].

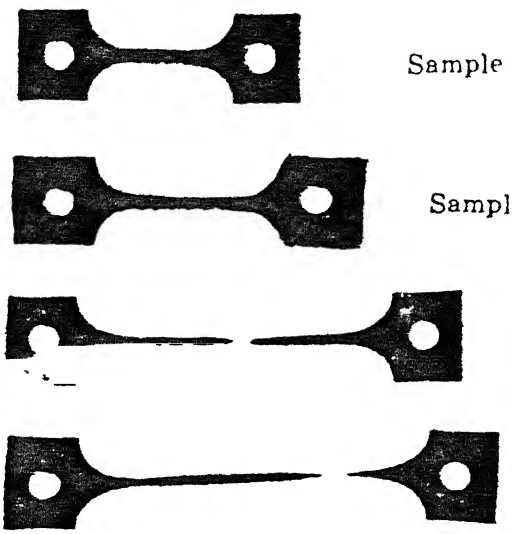

Sample No 1 Original

Sample No.2 $\varepsilon = 100\%$

Sample No.3 $\dot{\varepsilon} = 4 \times 10^{-4}/s$, $\varepsilon_f = 240\%$

Sample No.4 $\dot{\varepsilon} = 1 \times 10^{-3}/s$ $\varepsilon_f = 332.8\%$

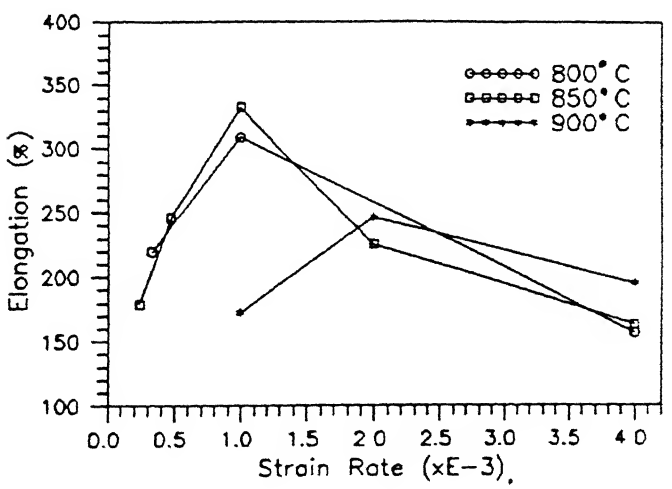

Fig.12 Superplastic behaviour in Fe_3Al-2Ti alloy.

CHAPTER 3

EXPERIMENTAL PROCEDURES

The prime aim of this work was to understand the hydrogen embrittlement of novel intermetallic iron aluminides by studying the effects of :

i) thermomechanical treatments,

ii) heat treatments and

iii) alloying by those elements which induce surface passivity

All the experiments were designed and carried out with the above aim in mind.

3.1 MATERIAL

A Fe-28Al (Fe_3Al) pancake of diameter 120 mm and thickness 15mm was the starting material. The starting material was obtained from Defence Metallurgical Research Laboratory,(DMRL) Hyderabad. This pan cake was processed via ingot metallurgy route. In order to minimize segregation, this pancake was homogenized at 1000°C for 4 hours.

3.2 THERMOMECHANICAL AND HEAT TREATMENTS

It is very well known that by altering the processing parameters, the properties of a given material can be changed (Figure 13).

Thermomechanical treatments (TMT) were designed to process the starting material in three different phase fields. The effect of recrystallisation and ordering treatment were also studied. All TMTs and the heat treatments used in present study are shown

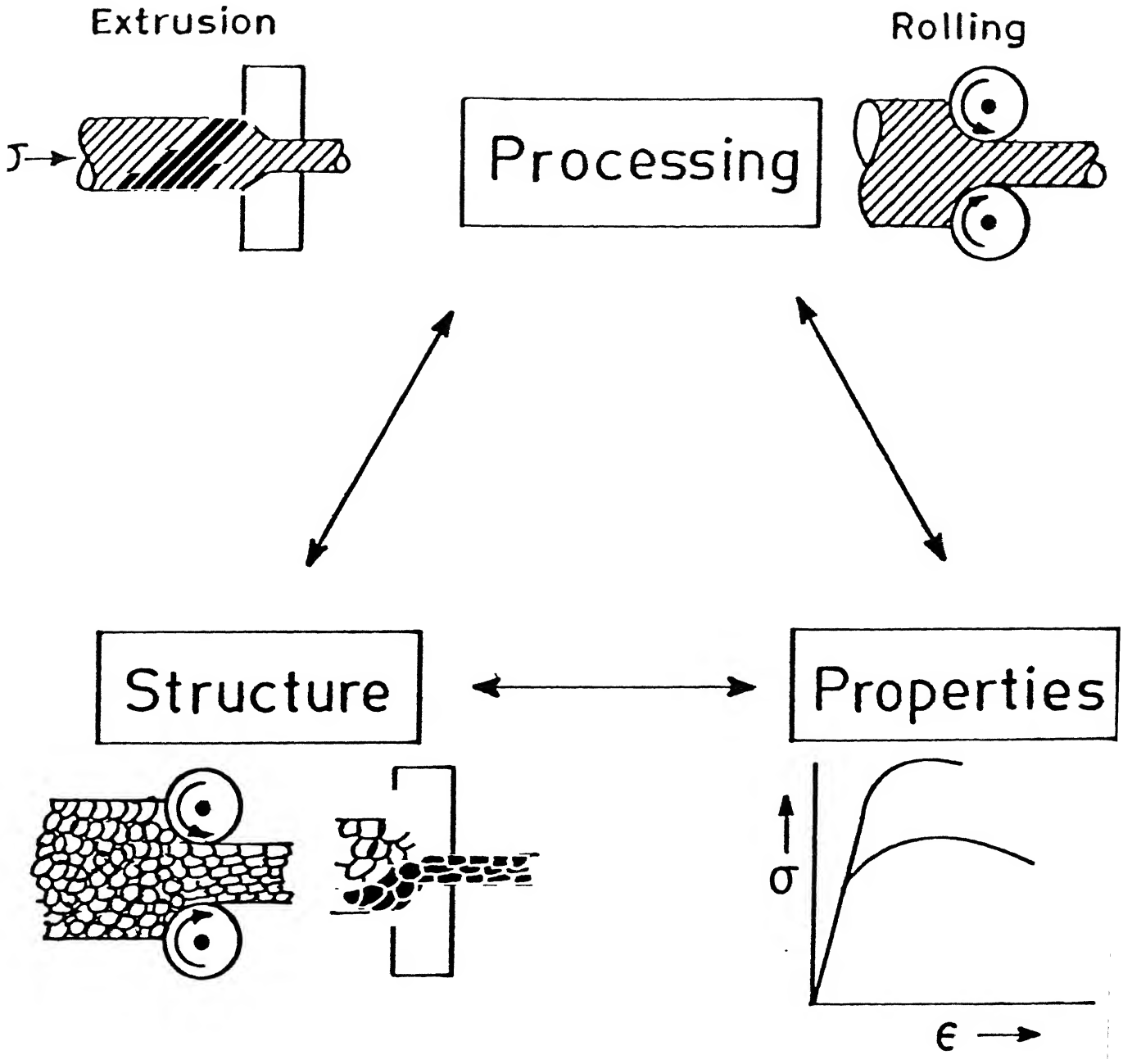

Fig.13 Correlation between processing-structure-properties.

in following flow sheet.

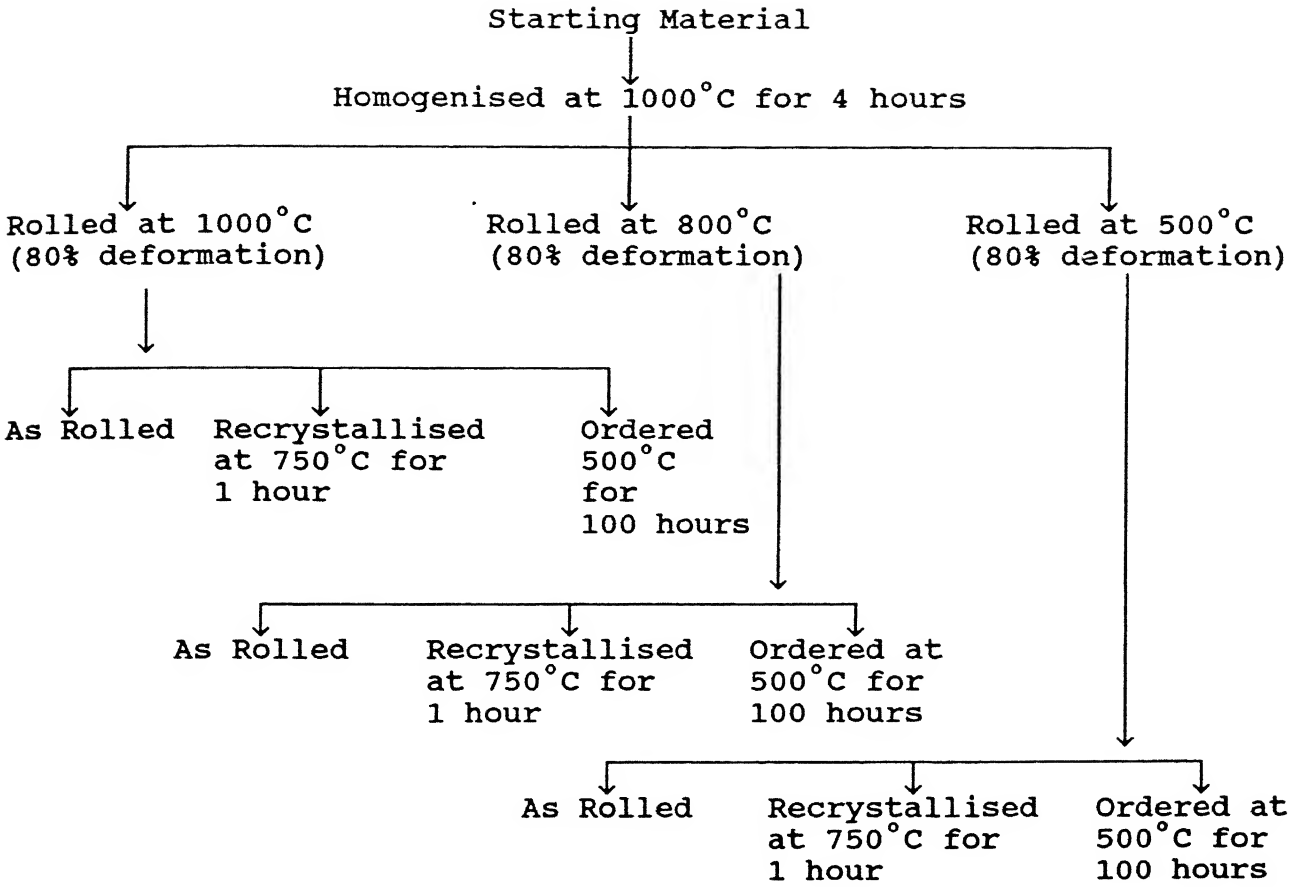

Rolling was carried out at 3 different temperatures namely 500°C, 800°C and 1000°C.The starting material for rolling had a thickness of 10 mm. They were processed at the following temperatures:

i) 1000°C (in disordered α phase field)

ii) 800°C (in ordered B2 phase field)

iii) 500°C (in ordered DO_3 phase field)

It was kept in the furnace for 1 hour for soaking. Soaking was carried out in air. Then it was rolled in multi passes to a strip of thickness 1.5 mm. This strip had a brown layer of oxide formed after rolling.

Tensile specimens of size 10mm x 5mm x 1.25mm were machined from these rolled strips. After establishing the recrystallisation behaviour of the rolled intermetallic, it was decided to recrystallise these tensile specimens at 750^{o}C for 1 hour in order to study the effect of recrystallisation on the room temperature mechanical behaviour.Ordering treatment of 100 hours at 500^{o}C was given to the rolled intermetallic in order to obtain the DO_3 crystal structure and study its effect on HE. Tensile specimens were encapsulated in vacuum to prevent oxidation during the ordering treatment. After all the TMTs and heat treatments, tensile specimens were polished on emery paper to remove the oxide film.

3.3 ALLOYED IRON ALUMINIDE

It is well known that certain elements additions to Fe promotes the formation of surface passive layer[25]. Table 7 shows the effect of such elements [25]. It has been recently suggested that inducing passivity in iron aluminides should reduce hydrogen reduction rates on iron aluminide surfaces and should minimise HE [14]. On this basis, the following elements were chosen for alloying in Fe_3Al. These elements were Cr, Mo, Ti, Ta, Nb, V, Ni and Si. 5 atomic percent of each element (of purity 99.99%) was added to binary Fe_3Al to make eight new alloys of type Fe_3Al-M (M = passivity inducing element). These alloys were melted in an arc furnace in an inert (argon) environment. Each alloy button was melted thrice to minimize segregation. These alloys were finally obtained in the shape of buttons. These buttons were homogenized at 1000^{o}C for 4 hours, before processing,

Table 7 . Effect of alloying elements on the characteristic points of the potentiostatic curve of iron.

Alloying Element	i_p	i_{cp}	E_{pp}	E_{cp}	E_f	E_t
Cr	increase	decrease	increase	increase	decrease	S N D
Mo	decrease	increase	No Data	increase	decrease	S N D
Si	No Effect	decrease	No Effect	increase	decrease	decrease
V	decrease	increase	No Effect	No Effect	decrease	S N D
Ti	decrease	No Data	No Data	No Data	No Data	No Data
Nb	decrease	No Data	No Data	No Data	No Data	No Data

i_p = Passivation Current Density

i_{cp}= Complete Passivation Current Density

E_{pp}= Passivation Potential

E_{cp}= Complete Passivation Potential

E_f = Film Break Through Potential

E_t = Transpassive State Potential

S N D = Shift In Negative Direction

to further minimize segregation.

All buttons were processed according to the following flow sheet:

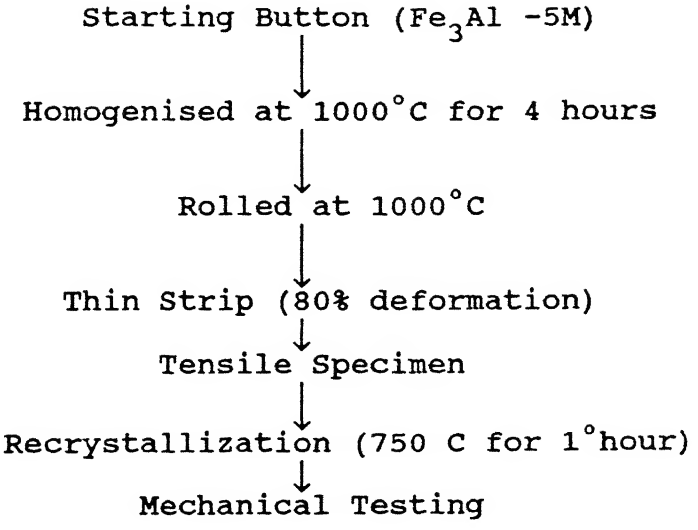

It was observed that only Fe_3Al-5Cr and Fe_3Al-5Ti could be rolled to 80% deformation in multiple passes. The Fe_3Al-5Ta intermetallic cracked after 50% deformation. The Fe_3Al-5Nb intermetallic cracked after 40% deformation. The Fe_3Al-5Mo, Fe_3Al-5Si and Fe_3Al-5V could not be rolled as they cracked in the first rolling pass itself. Therefore, tensile specimen could be made out of only Fe_3Al-5Cr and Fe_3Al-5Ti strips.

3.4 MATERIAL CHARACTERIZATION

3.4.1 MICROHARDNESS MEASUREMENTS

Microhardness measurements of specimens were performed using a Carl Zeiss Jena "Vertival" optical microscope attached with a microhardness tester.Observations of indentations were made at magnification of 25X. A load of 100 grams was used for all studies. All the values are noted as Vicker's Hardness Number (VHN) which was obtained from

$$VHN = \frac{1854.4P}{d^2}$$

where P = load in gms

d = diameter of indentation mark in μm

3.4.2 X-RAY DIFFRACTION (XRD)

XRD patterns of Fe_3Al and Fe_3Al-M intermetallics were recorded after different thermomechanical treatments with a Rich-Siefert 2002 X-ray diffractometer using CuK_α radiation. The specimens were in the form of strips in the case of thermomechanically treated and alloyed intermetallics.

3.4.3 MICROSCOPY

The samples at different stages (processing, heat treatment and mechanical testing) were observed for their microstructure. Optical microscopy was performed using Leitz Laborlux 12 MES microscope at a magnification of 100.

The main problem faced in optical microscopy was the choice of a suitable etchent for revealing the structure of binary Fe_3Al. Several etchents (listed below) were tried, some with partial success and others without any success.

1)	CH_3COOH	25 ml	
	HNO_3	15 ml	No success
	HCl	15 ml	
	WATER	5 ml	
2)	GLYCERIN	75 ml	
	WATER	15 ml	No success
	HNO_3	5 ml	
	HF	5 ml	
3)	HNO_3	5 ml	

	HF	5 ml	No success
	WATER	15 ml	
4)	HCl	20 ml	Partially successful [26]
	HNO_3	5 ml	
5)	CH_3COOH	8 parts (by volume)	Fully successful [22]
	HNO_3	4 parts (by volume)	
	HCl	1 parts (by volume)	

Several compositions of the first four mentioned etchents were tried but they did not reveal grain boundaries. The etchent which revealed grain boundaries and hence microstructure of Fe_3Al in a reproducible manner was the last mentioned etchent [22]. Using this etchent it was noticed that etching should be done only for few seconds (5-15 sec) as etching for longer times caused etch pit formation.

Electrochemical etching was also performed with the following etchent. The etchent was prepared by dissolving 25gm of CrO_3 in 133ml of CH_3COOH and 7ml of water at 60-70^{o}C. Etching was done under the following electrochemical conditions :

Current density = 0.09 - 0.22 Amp/cm^2

Voltage (d.c.) = 20 volts

Temp^{o}(C) = 17-19^{o}C

Etching Time = 4-5 minutes

As lot of heat was evolved during electrochemical etching, the electrolyte was kept in ice cooled bath. Electrochemical etching was partially successful in revealing cracks and inclusions but did not reveal grain boundaries. Grain size measurement was carried out using line intercept method.

All the fractured tensile specimens were examined under scanning electron microscope (JEOL JSM 840 A). In order to study the nature of fractographic cleavage planes, the fracture surfaces were studied in 2 conditions

i) etched and

ii) unetched

Here the aim of etching was to reveal the nature of planes by observing dislocation pit shapes. Etching of the previously observe fracture surface was performed for 1 minute by etchent mentioned last in above section. The etch pits were observed in the SEM to reveal the crystallographic nature of the cleavage planes on the fracture surface.

3.4.4 MECHANICAL TESTING

Tensile testing was done on INSTRON Testing machine at a constant strain rate of 10^{-4} sec^{-1}. All the tests were carried out in air at room temperature. The tensile samples were coated with silicon oil to prevent hydrogen entry into the lattice during straining[27].

CHAPTER 4

RESULTS AND DISCUSSION

4.1 MATERIAL CHARACTERIZATION

The material used in the present study Fe-28Al was received in the form of a pan cake from DMRL, Hyderabad of diameter 120mm and thickness 15 mm. It was processed by the ingot metallurgy route. The results of the characterization studies conducted on the as-received and processed intermetallic are presented and discussed below.

4.1.1 Microhardness

The microhardness of the as- received intermetallic was 225 VHN (Figure 14). On comparing this with thermomechanically treated Fe_3Al, it can be concluded that the as- received intermetallic was softer (Figure 14). The as-received intermetallic had not undergone any deformation process and so its as-cast structure is indicated by the low hardness value. There is a steep rise in microhardness of the rolled intermetallic as compared to the as-received intermetallic (Figure 14). However, the difference in microhardness of intermetallics rolled at the three different temperatures was not very significant. The rolled intermetallic exhibited a hardness of around 390 VHN. In fact, rolled strips were very hard and it was very difficult to section the thin 1.5 mm strips using a high speed steel blade.

This increase in hardness can be explained by the high dislocation density created due to deformation processing and also

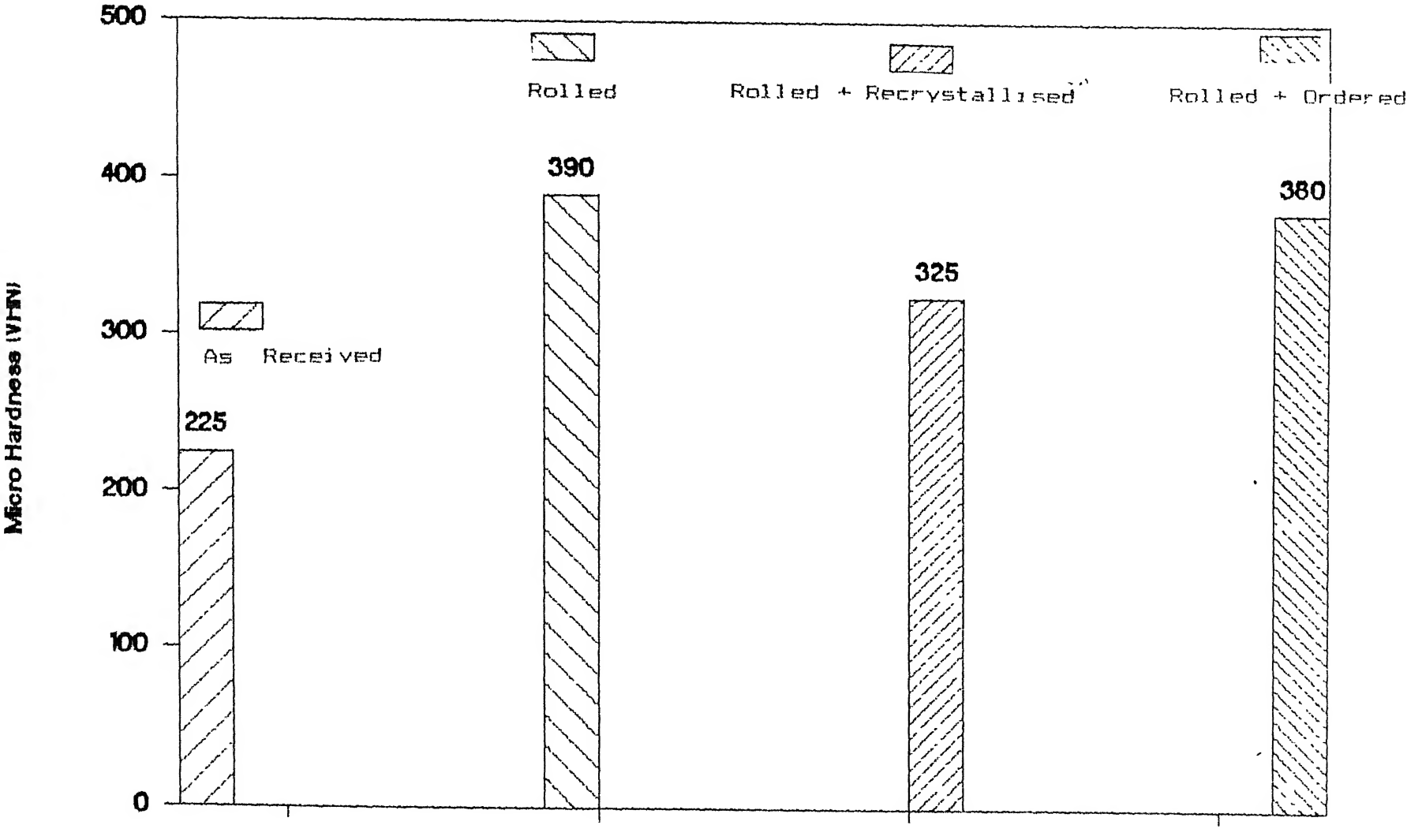

Fig.14 Microhardness of Fe_3Al after different processing stages

cooling rate effects [28]. After quenching the rolled intermetallic from high temperature, it retains a high vacancy concentration. These quenched in vacancies interact with dislocations and form dislocation loops which result in increased hardness. In this regard, Baker and Nagpal have shown that water quenched iron aluminide had the highest hardness due to the highest cooling rate employed [28]. Moreover, the rolled intermetallic has a high dislocation density due to heavy deformation imparted to it. Thus, it can be concluded that water quenching and heavy deformation (80%) were responsible for an increase in the hardness of the rolled intermetallic compared to the as-received intermetallic. The microhardness of the rolled and recrystallised intermetallic was lower than that of the rolled intermetallic (Figure 14). This is expected as there was a reduction in dislocation density because of annihilation of dislocations and vacancies during annealing. Therefore, reduced hardness was obtained after recrystallisation. However, there was no significant variation in the microhardness of intermetallic rolled at 3 different temperatures and then recrystallised.

The microhardness of the rolled +ordered intermetallic was greater than the rolled +recrystallised intermetallic (Figure 14). This is attributed to the presence of ordered DO_3 structure. The presence of DO_3 structure after ordering treatment has been later confirmed in this study and this would be presented later. Therefore, hardness increased after the ordering treatment of 100 hours at 500°C.

Fe_3Al-5Ti has a microhardness value of 495 VHN after rolling. This is a very hard intermetallic as compared to Fe_3Al-5Cr intermetallic (Figure 15). The higher hardness of Fe_3Al-5Ti could be attributed to its higher degree of strain hardening.

4.1.2 XRD Analysis

The XRD pattern of the as-received intermetallic is shown in Figure 16. It showed peaks of fundamental reflection such as (220), (400), (422), (440) and (620) characteristic of the BCC iron aluminide structure. It was observed that h, K, and l were all even for fundamental reflections and that there was no peak when h+K+l was odd [29]. This confirmed that the material had a BCC crystal structure. No superlattice peak such as (111), (311) or (331) were observed. Hence, it can be deduced that this intermetallic had the disordered α structure.

The XRD pattern of the rolled intermetallic is shown in Figure (16). It is noteworthy that XRD patterns of material rolled at three different temperature did not exhibit any significant variation. All the peaks for the rolled condition corresponded to the disordered α structure.

The X-ray diffraction pattern after the ordering treatment are presented in Figure (16). The DO_3 superlattice reflection such as 111, 311, 311 etc could not be still observed after ordering. Possible reason could be because these peaks were of very low intensity and could be observed only after a high degree of ordering. Although the absence of DO_3 superlattice peaks could suggest that transformation to DO_3 phase has not been completed, there was another evidence which confirmed the presence of DO_3

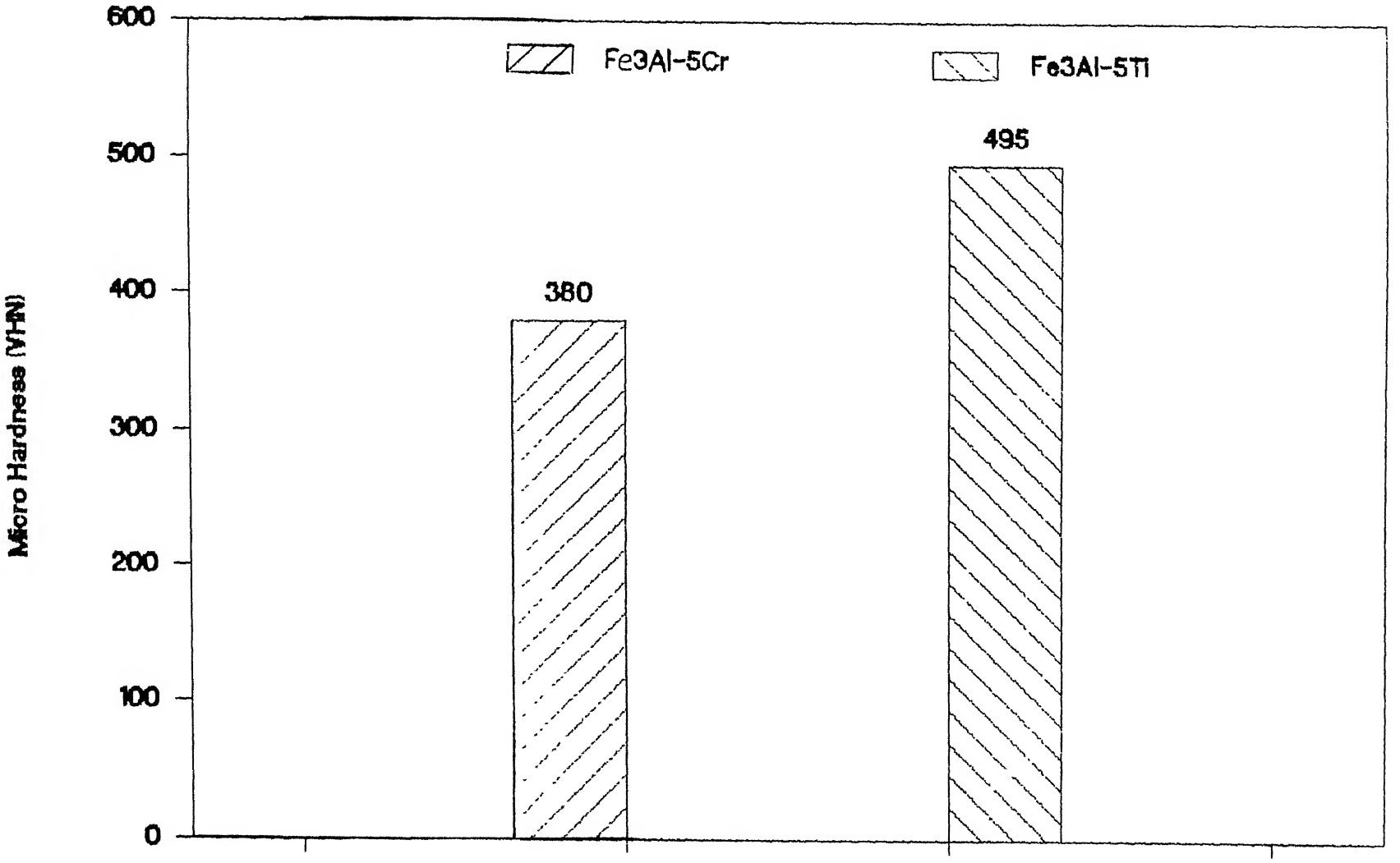

Fig.15 Microhardness of Fe_3Al-5Cr and Fe_3Al-5Ti intermetallics after rolling at 1000°C and recrystallised at 750°C for 1 hour.

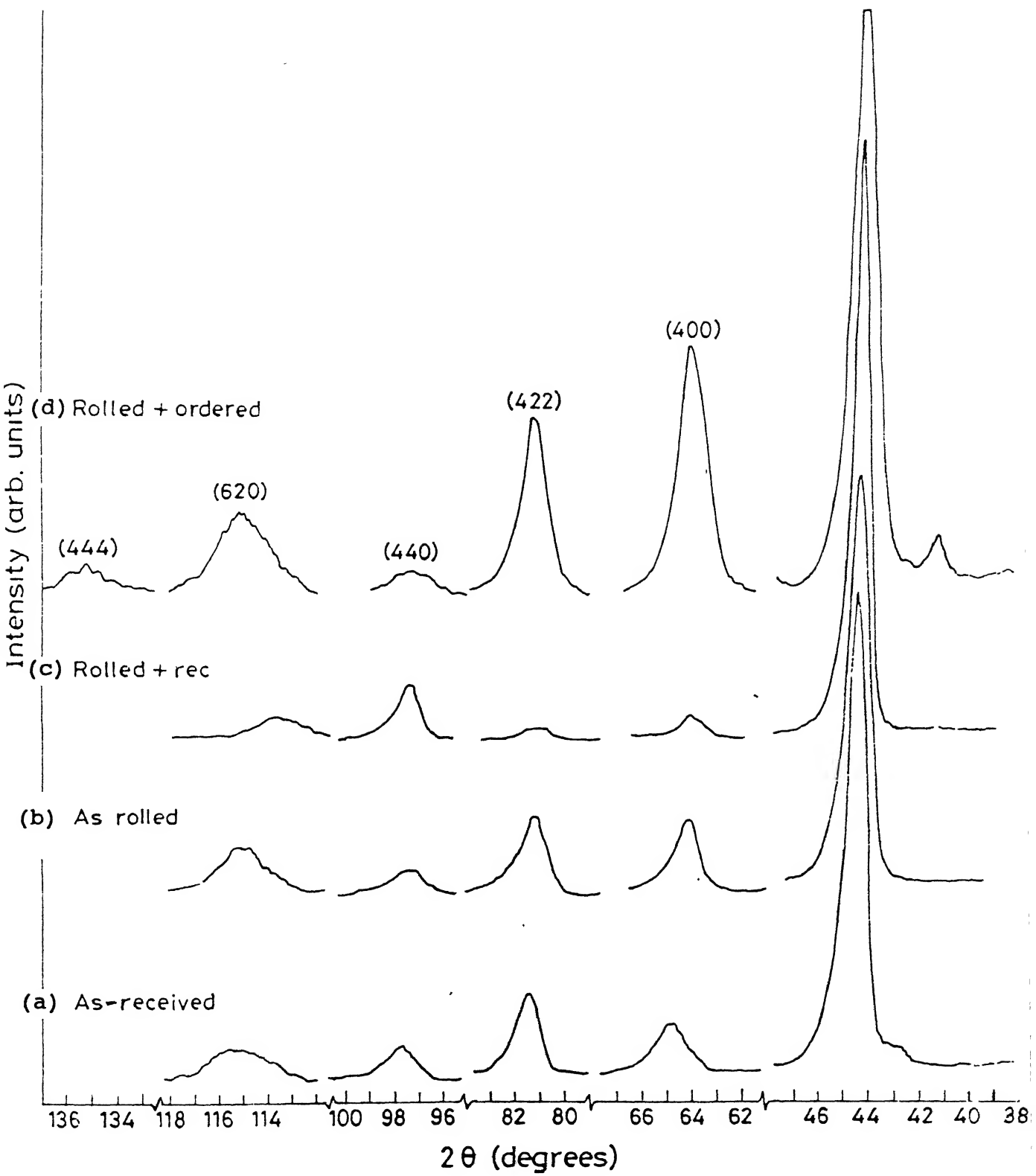

Fig.16 XRD patterns of Fe_3Al: (a) as-received (b) rolled at 1000°C to 80% deformation (c) rolled at 1000°C to 80% deformation + recrystallised at 750°C for 1 hour (d) rolled at 1000°C to 80% deformation + ordered at 500°C for 100 hours

phase. A special attention should be paid to the behaviour of 440 fundamental line of the Fe_3Al alloy. On careful observation of Figure (16), it can be seen that the 440 peak in the ordered material is much wider. Oki et al. elucidated the process of ordering[30]. It was concluded that the ordering takes place by the nucleation and growth of DO_3 domains. The final state of order was attained by coalescence of ordered domains. Oki et al. regard this broadening of the 440 peak as due to the coexistence of two phases whose lattice parameters are significantly different[30]. Thus, broadening of the 440 fundamental line confirmed the presence of DO_3 phase. At the ordering temperature of 500°C, presence of both the α and DO_3 phases was indicated. The XRD pattern of ordered iron aluminide also showed an extra peak at 2θ = 41.4. However, this peak does not correspond to any reflecting plane in cubic system and this peak has not been indexed in Figure 16. The nature of XRD pattern was very similar for intermetallic rolled at three different temperatures and then ordered.

The XRD patterns of Fe_3Al-5M type of intermetallics are shown in Figure 17. It was observed that iron aluminide alloyed with Mo, V and Nb showed similar reflections. It was interesting to note that all the peaks of Fe_3Al-5Mo, Fe_3Al-5V and Fe_3Al-5Nb matched with the fundamental peaks of binary iron aluminide Fe_3Al. However, the XRD pattern of Fe_3Al-5M type intermetallic exhibits a variation in (440) peak width. XRD pattern of Fe_3Al-5Mo, Fe_3Al-5V and Fe_3Al-5Nb showed a broader (440) peak suggesting that some kind of order was present in these alloyed iron aluminides [30].

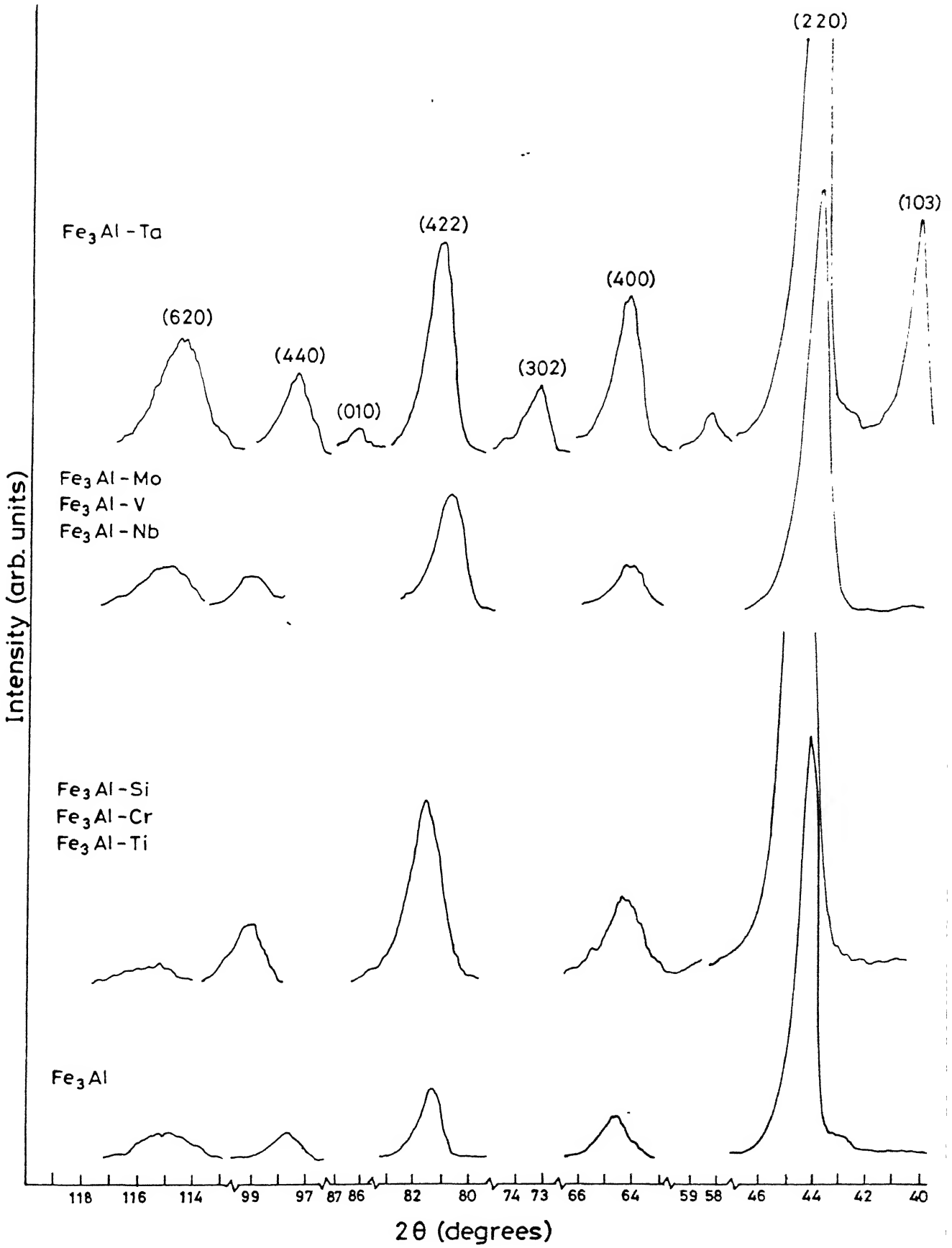

Fig.17 XRD patterns of Fe_3Al-5M intermetallics.

McKamey and Horton have proved earlier that addition of certain alloying elements to Fe_3Al elevates its critical ordering temperature [21]. Addition of Mo, V and Nb to iron aluminides could lead to some degree of ordering during the deformation process at high rolling temperature of 1000°C. This has been reflected by broadening of the (440) peak. However, Fe_3Al-5Ta, Fe_3Al-5Ti, Fe_3Al-5Cr and Fe_3Al-5Si intermetallics did not exhibit significant (440) peak broadening. This suggests that only Mo, V and Nb additions have lead to some degree of ordering in these iron aluminides. Table 8 presents the measured 2θ values from XRD pattern of Fe_3Al-5M intermetallics using CuK_α radiation.

The XRD pattern of Fe_3Al-5Ta showed several additional peaks (ie at 2θ = 40.4, 58.4, 73.4 and 87.5) apart from those corresponding to Fe_3Al which suggests the formation of other intermetallic phases. Peaks indexed as (103) and (302) in Figure 17 belong to Fe_5Ta_3 intermetallic, while the peak marked (010) corresponds to Al_3Ta_2 intermetallic. However, the peak at 2θ = 58.4 could not be indexed.

4.1.3 Optical Microscopy

The as-received intermetallic did not reveal any grains after polishing and etching (Figure 18). Grain boundaries could not be etched and revealed due to possible macrosegregation in the as-received intermetallic. Optical microscopy of the intermetallic after undergoing thermomechanical treatments would be discussed in the subsequent sections.

Table 8 2θ values from XRD patterns of Fe_3Al-5M intermetallics using CuK_α radiation.

Element	$(2\theta)_{220}$	$(2\theta)_{400}$	$(2\theta)_{422}$	$(2\theta)_{440}$	$(2\theta)_{620}$	Does(440) Broaden?
Ti	44.4	64.5	81.6	99.2	115.2	No
Cr	44.4	64.4	81.4	99.2	115.4	No
Si	44.2	64.5	81.4	99.4	115.4	No
V	44.0	64.4	81.1	99.2	115.2	Yes
Mo	44.2	64.3	81.2	99.2	115.2	Yes
Nb	44.4	64.4	81.1	99.2	115.2	Yes
Ta	44.5	64.4	81.4	97.5	114.5	No

Fig.18 Optical micrograph ofas-received intermetallic in polished and etched condition.

4.2 MECHANICAL BEHAVIOUR

4.2.1 Rolled Intermetallic

The as-received intermetallic was homogenised at 1000°C for 4 hours and then rolled at 3 different temperatures, namely 1000, 800, and 500°C. The results of room temperature tensile test conducted on the rolled intermetallic are presented in Table 9.Tensile tests were duplicated in order to validate the authenticity of the tensile testing experiment. This has been shown by 2 values of mechanical properties for rolled intermetallic in Table 9. In this table the material rolled at 1000°C has been abbreviated as R1000.

The rolled intermetallic showed a gradual decrease in fracture strength with decreasing rolling temperature (Figure 19a). Ductility, as given by the plastic strain from the engineering stress-strain curve, was practically nil in all the three cases. Brittle or cleavage kind of fracture was revealed by SEM fractographs (Figure 20). This variation in the fracture strength can also be explained on the basis of optical microstructure of this material after the rolling treatments (Figure 19b,19c and 19d).

Figure 19(b) shows the optical microstructure of the intermetallic rolled at 1000°C. It exhibited very fine grains (marked by ⟶) and regions of elongated, deformed grains. These fine subgrains have nucleated as a consequence of dynamic recrystallisation and recovery process occurring at the high rolling temperature of 1000°C. Figure 19(b) also shows deformed long grain (marked by ↑) which has not completed the

Table 1 Room temperature tensile properties of Fe_3Al after thermomechanical and heat treatments.

Condition	Y. Strength (MPa)	UTS (MPa)	Ductility (%)	Fracture	Grain Size(μ)
R1000	830	840	0	Cleavage	28
R1000	795	810	0	Cleavage	28
R800	625	730	0	Cleavage	**
R800	610	710	0	Cleavage	**
R500	370	370	0	Cleavage	**
R500	350	350	0	Cleavage	**
R1000+Rec	380	460	1.4	Cleavage	295
R800+Rec	580	570	0	Cleavage	140
R500+Rec	670	730	0.9	Cleavage	90
R1000+Ord	565	560	0	Cleavage	155
R800+Ord	455	455	0	Cleavage	340
R500+Ord	360	360	0	Cleavage	720

** Grain size measurements were not possible in these cases because of highly deformed and elongated structure [Figure 19(c) & 19(d)]

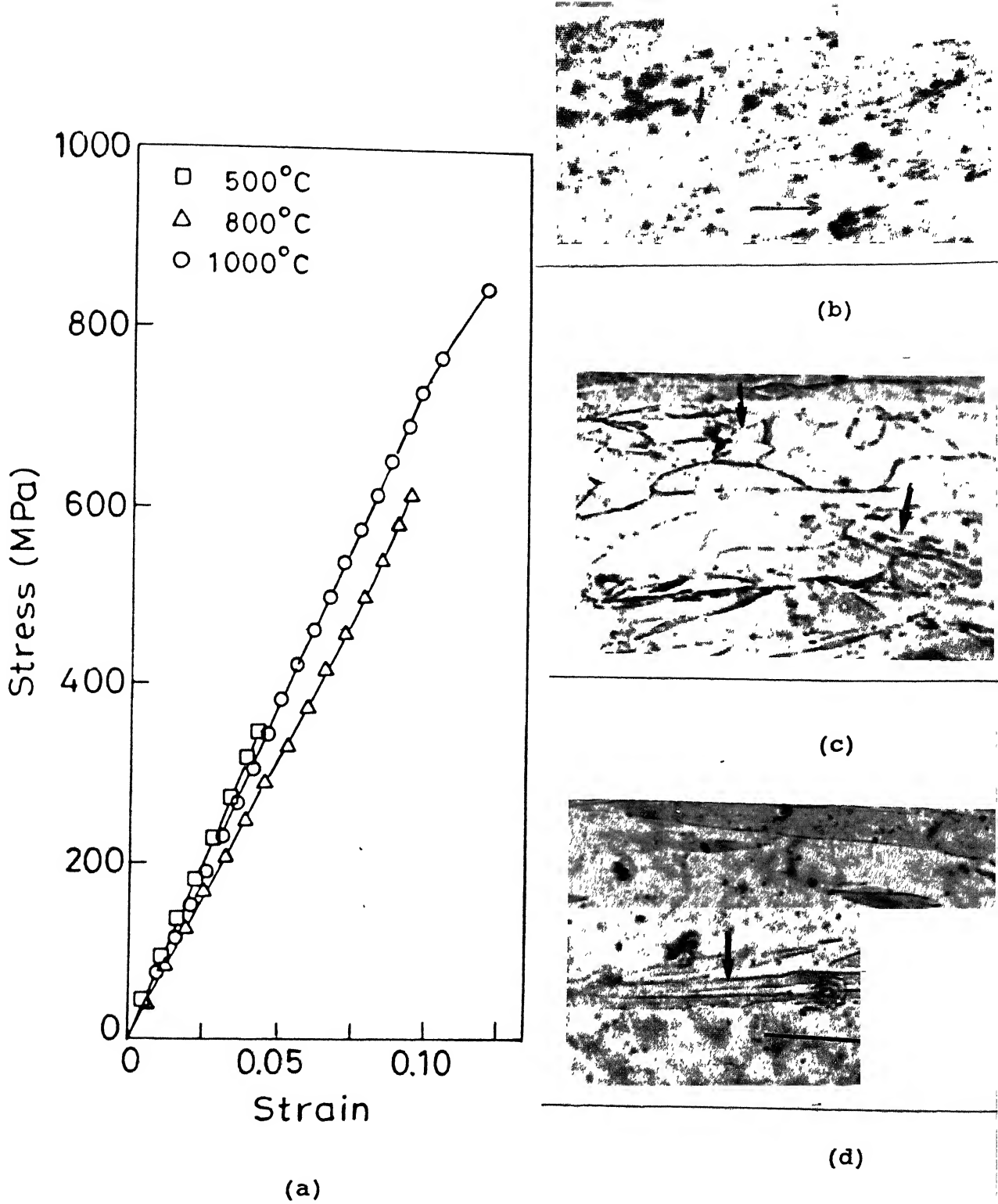

Fig.19 (a) Stress-strain behaviour of rolled intermetallic and optical micrographs of Fe_3Al rolled at (b) 1000°C, (c) 800°C and (d) 500°C.

recovery/recrystallization process. Figure 19(c) shows the optical microstructure of the intermetallic rolled at 800°C. Apart from a few recovered subgrains (marked by ↓), it exhibited mainly deformed, coarse and elongated grains which had partially undergone dynamic recrystallisation. Figure 19(d) shows the optical microstructure of the intermetallic rolled at 500°C. It shows highly deformed, coarsest grain structure with stringer type of long grains (marked by ↓). This intermetallic had not undergone dynamic recrystallisation at the low rolling temperature of 500°C. It is quite possible that it was just in the initial stages of recrystallisation as a small number of subgrains could be identified (marked by ⟶). According to Hall-Petch theory, this change in grain size after the rolling treatment at different temperatures could be used to explain the variation in fracture strength of iron aluminides.

Another strengthening mechanism has been proposed by Morris and Leboeuf [31]. Morris and Leboeuf have concluded that the subgrains boundaries in deformed iron aluminides were composed of immobile <100> dislocations [31]. These subgrains help in distributing strain uniformly within the material resulting in higher strengths. In the present study, it has been observed earlier that intermetallic rolled at 1000°C has the largest subgrain boundary area, thereby resulting in higher fracture strengths compared to the intermetallic rolled at 800°C and 500°C.This experimental result indirectly validate Morris and Leboeuf's theory.

Another possible reason for this variation could be explained on the basis of different phases present in the material. Though there is no evidence of other phases apart from the α phase from XRD patterns of material rolled at 500, 800 and 1000°C (Figure16), this could be due to the low volume fraction of other phase(s).The intermetallic rolled at 1000°C has a disordered BCC structure. However,there could be some amount of $\alpha \longrightarrow$ B2 transformation while soaking the intermetallic at800°C. This intermetallic may have disordered B2 phase present in addition to α. On similar lines, it could be argued that the intermetallic rolled at 500°C could have a mixture of disordered α, B2 and DO_3 phase(s). Their amount could be so small that they were not revealed by any superlattice peak by X-ray diffraction technique

Figure 20 (a), (b) and (c) show transgranular or cleavage kind of fracture morphology in all the three cases in unetched condition. Figure 20(b) and 20(c) shows somewhat irregular cleavage surface. Figure 20(a) shows river line pattern (marked by ↑). These river patterns were formed as a consequence of convergence of irregular cleavage faces [32]. These rivers have a curvilinear shape (as evident from SEM fractograph), running parallel to each other. These rivers often form due to presence of screw dislocations [32]. It is interesting to note that Morris and Leboeuf have shown that subgrain boundaries of iron aluminide were composed of <100> dislocations which were of screw orientation [31].

Figure 20(d), (e), and (f) shows fracture morphology after etching the fracture surfaces of intermetallic rolled at 1000°C,

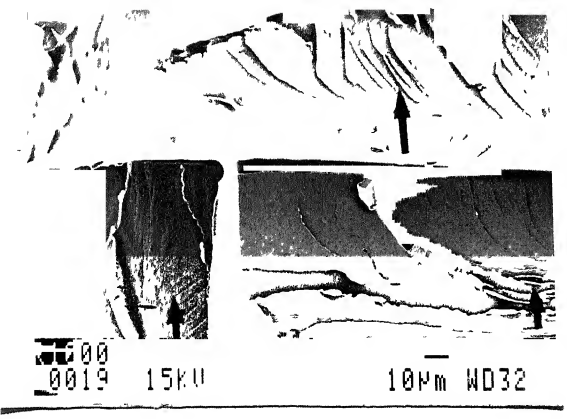

(a)

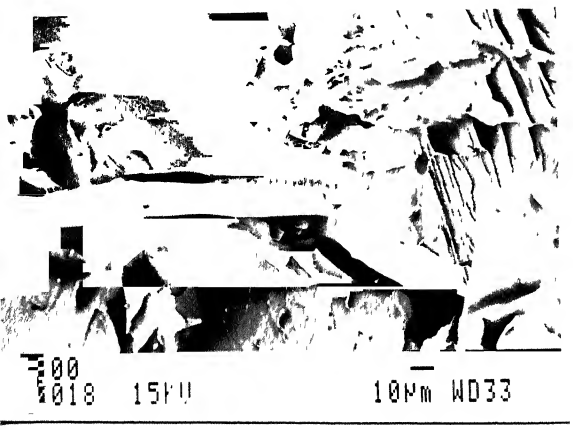

(b)

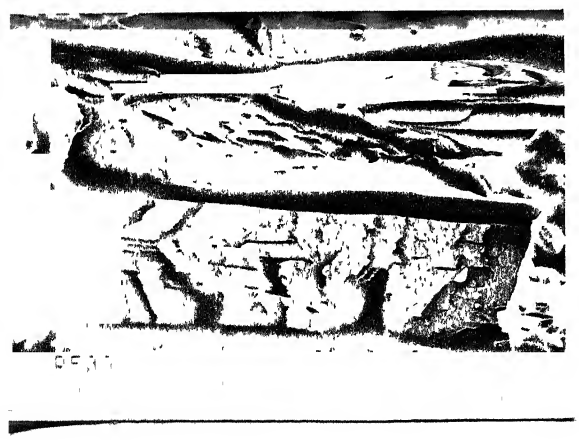

(c)

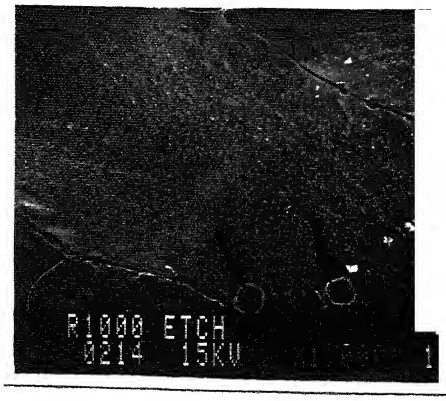

(d)

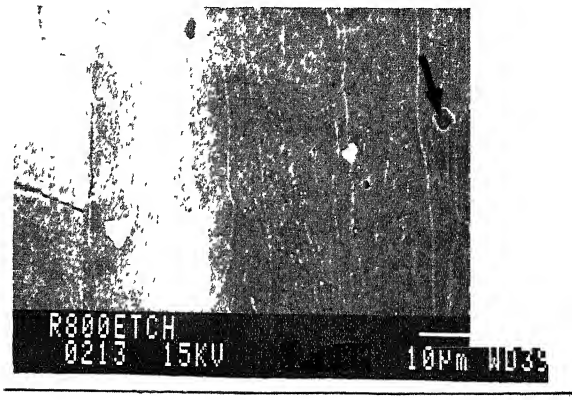

(e)

(f)

Fig.20 Fracture morphology of iron aluiminide rolled at (a) 1000°C unetched, (b) 800°C unetched, (c) 500°C unetched, (d) 1000°C etched, (e) 800°C etched and (f) 500°C etched.

800°C and 500°C respectively. It is well known that emerging points of dislocations can sometimes be observed by suitable chemical etching [33]. Since the lattice around the dislocations is in highly strained state, it is preferentially attacked by etchant which dissolve away surface atoms and the resulting etchpits can be observed.

A large number of features were revealed in the SEM fractographs, after etching of Fe_3Al samples. At a magnification of 1000X, it was more clear that most of the etch pits were of rectangular shape [Figure 20(d) and 20(e)] (marked by ↓). Rectangular etch pits indicate that the cleavage plane was of cube type, for example, {100}.

A possible reason for the observation of {100} cleavage planes under embrittlement conditions could be the following.

Mobile dislocations trap hydrogen and carry it along with them to potential flaw sites such as crack tips, inclusions and voids. Generally, in intermetallic structures, dislocations are in form of partials. Fe_3Al has a high stacking fault energy (SFE) value of 500 ergs/cm^2 [34]. Thus it forms partial dislocations with a low splitting width, which are very difficult to observe. These hydrogen containing partial dislocations glide on the slip planes in the ordered B2 and DO_3 structures of iron aluminides and can be locked as immobile <100> dislocations by the Freidel mechanism [34]. According to most of the accepted theories of hydrogen embrittlement, hydrogen should exceed a critical concentration at potential flaw sites, to cause embrittlement. Critical hydrogen concentration is a function of stresses

generated by hydrogen occupying tetrahedral interstitial sites on the {100} planes of the ordered B2 and DO_3 structure. The actual number of tetrahedral interstitial sites would depend on the crystal structure (B2 or DO_3) but there are enough interstitial sites which leads to hydrogen concentration and finally crack initiations by decohesion mechanism.

Slip bands were also observed for the intermetallic rolled at 800°C by this study [Figure 20(f)]. Moreover, typical feature of dislocation loop is observed in Figure 20(d). The large plastic strain around cracks or indentations are produced by small "punching" dislocation loops (marked by ⟶) along crystallographic directions suitable for slip. This is analogous to dislocation loop appearing as pairs of etch pits along [100] and [110] directions for an indentation on the (100) plane of MgO [33].

All arc melted buttons of Fe_3Al-5M intermetallics were homogenised at 1000°C for 4 hours and then rolled at 1000°C. Rolling lead to cracking in most of the Fe_3Al-5M intermetallics. Rolling schedule was carried out to give 80% deformation in multi passes. The results of rolling are provided below:

Fe-26Al-5 Cr	Rolled successfully to produce 80% deformation
Fe-26Al-5Ti	Rolled successfully to produce 80% deformation
Fe-26Al-5Ta	Rolled successfully to produce 50% deformation and then cracked
Fe-26Al-5Mo	Cracked in first pass
Fe-26Al-5Nb	Rolled successfully to produce 40% deformation and then cracked

Fe-26Al-5V Cracked in first pass

Fe-26Al-5Si Cracked in first pass

The possible reasons for the failure in rolling could be due to two reasons. Firstly, the alloying element could have been added in excess. 5 atomic % addition might have shifted the phase boundaries into zones of brittle phases and hence cracking could occur. Moreover, the alloying additions could have lead to segregation and caused cracking. Secondly alloying would have lead to formation of complex brittle intermetallic systems apart from iron aluminides. The complex system(s) could cause cracking during rolling. Akdeniz et al. validated the above reasoning for the Fe-Al-Si system [35]. Addition of Si to the Fe-Al system retarded the formation and growth of intermetallic via the initial formation of a thin layer of $Fe_xSi_yAl_z$ at the interface. This $Fe_xSi_yAl_z$ acted as a barrier to diffusion and restricted the formation of Fe-Al compounds and lead to cracking during processing.. Although the XRD analysis of Fe_3Al-5M intermetallics did not reveal the presence of additional intermetallic phases (except in the case of Fe_3Al-5Ta), it is quite possible that some additional phase(s) form(s) in a small amount which could not be identified by XRD analysis. Perhaps, This could be the reason for cracking for other Fe_3Al-M alloys.

These alloys need to be studied in greater detail for further explanation of the cracking phenomena during rolling.

4.2.2 Rolled and Recrystallised Intermetallic

Recrystallisation processes vary greatly in Fe_3Al system with several variables such as TMTs, alloying, crystal structure and

microstructure[4]. Thus it is very difficult to predict precisely the recrystallization temperatures and kinetics in the Fe_3Al system. The recrystallisation behaviour of the iron aluminide was studied in accordance with McKamey and Pierce's earlier study [18]. McKamey and Pierce had suggested that partially recrystallised microstructure results in highest ductility. Partially recrystallised microstructure exhibits less grain boundary area. The grain boundaries are the proposed site for H ingress into the material. Thus, according to them, reduction in grain boundary area leads to an increase in ductility.

In order to establish recrystallization schedule for mechanical testing purposes, the intermetallic rolled at 500°C was annealed at 750°C for 1/2 hour, 1 hour and 2 hours to establish the hardness as a function of recrystallisation time. Figure 21(a) shows the variation in hardness as a function of recrystallization time. Microhardness studies showed that hardness decreased with increasing recrystallisation time at 750°C. This could be explained by annihilation of dislocations during annealing. The difference in microhardness after 1/2 hour and 1 hour of recrystallization was not very great. Figure21(b) shows the intermetallic annealed for 1/2 hour at 750°C. It exhibits nucleation of subgrains as a consequence of recovery process (marked by $\longrightarrow$). Figure 21(c) shows the intermetallic annealed at 750°C for 1 hour. It exhibits a partially recrystallised microstructure ie. consisting of recovered subgrains and equiaxed recrystallised grains. Figure 21(d) shows a recrystallised, equiaxed grain structure as a consequence of

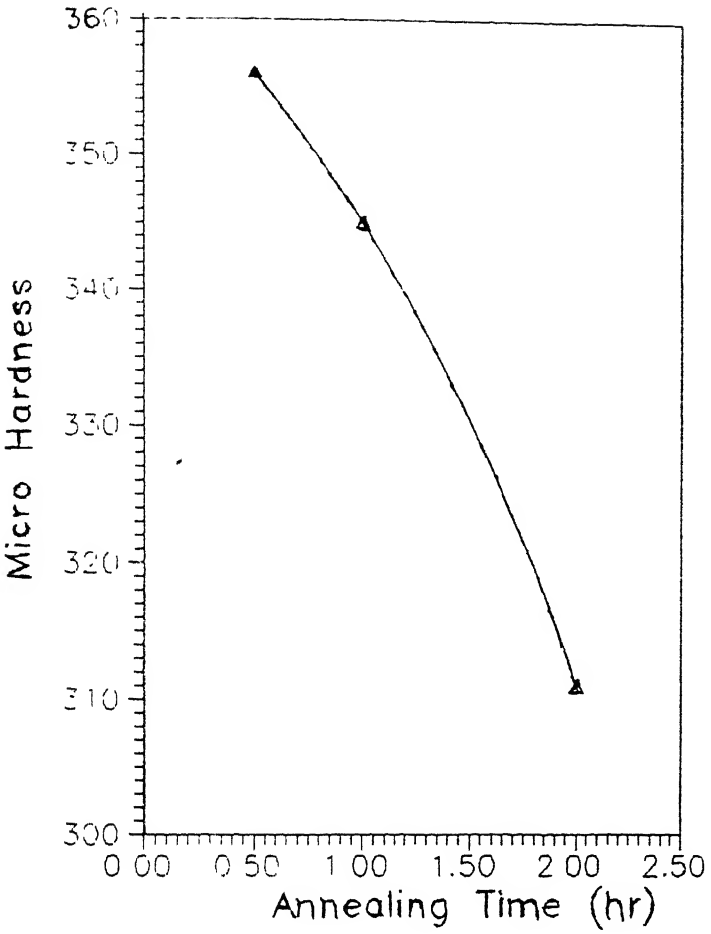

(a)

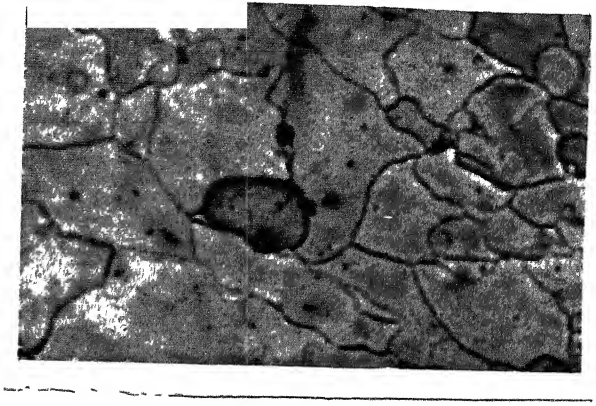

(b)

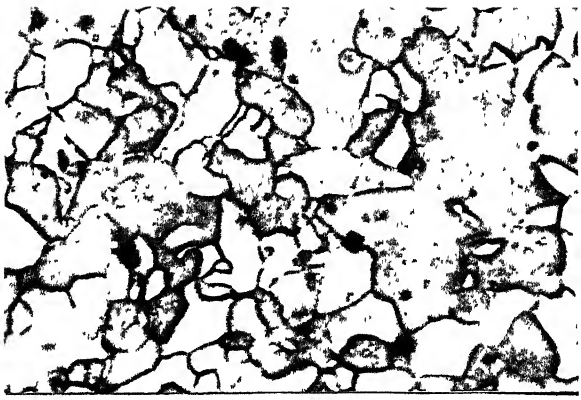

(c)

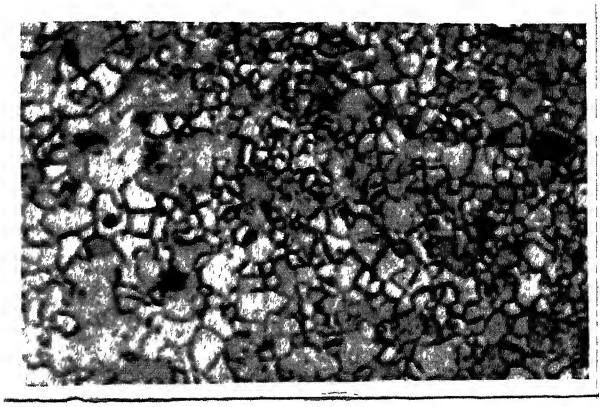

(d)

Fig.21 (a) Microhardness as a function of annealing time at 750°C for initially intermetallic rolled at 500°C and optical micrographs of same intermetallic annealed for (b) 1/2 hour, (c) 1 hour and (d) 2 hours at 750°C.

annealing for 2 hours. The rolled material annealed for 1 hour at 750°C resulted in a partially recrystallised microstructure. Therefore, 1 hour was chosen as recrystallising time in the present study. McKamey and Pierce have suggested that partially recrystallised microstructure suppresses HE [18].

Figure 22(a) shows the engineering stress-strain curve for the intermetallic rolled at three different temperatures and then recrystallised at 750°C for 1 hour. All the salient features of tensile testing are presented in Table 9. A significant change in fracture strength was observed for the different intermetallics. The intermetallic rolled at 500°C exhibited the highest fracture strength of 730 MPa while the intermetallic rolled at 800°C and 1000°C showed lower fracture strengths of 570 MPa and 460 MPa, respectively.

Fracture morphology has been presented in Figure 23. Fracture morphology reveals cleavage kind of brittle fracture, similar to that observed for the rolled intermetallic. Figure 23(b) and (c)shows irregular cleavage surfaces, with river pattern in different grains (marked by ↑). However, Figure 23(a) exhibits predominantly river flow pattern. In etched condition, fractographs reveal rectangular etch pits suggesting that the cleavage plane was of cube type. Figure 23(d) shows some characteristic protruding features (marked by X). These are also etch pits. However, the side of etch pits have been also dissolved that it superficially appears as protruding features.

The variation in fracture strength after the rolling and recrystallization treatments can be explain on the basis of grain

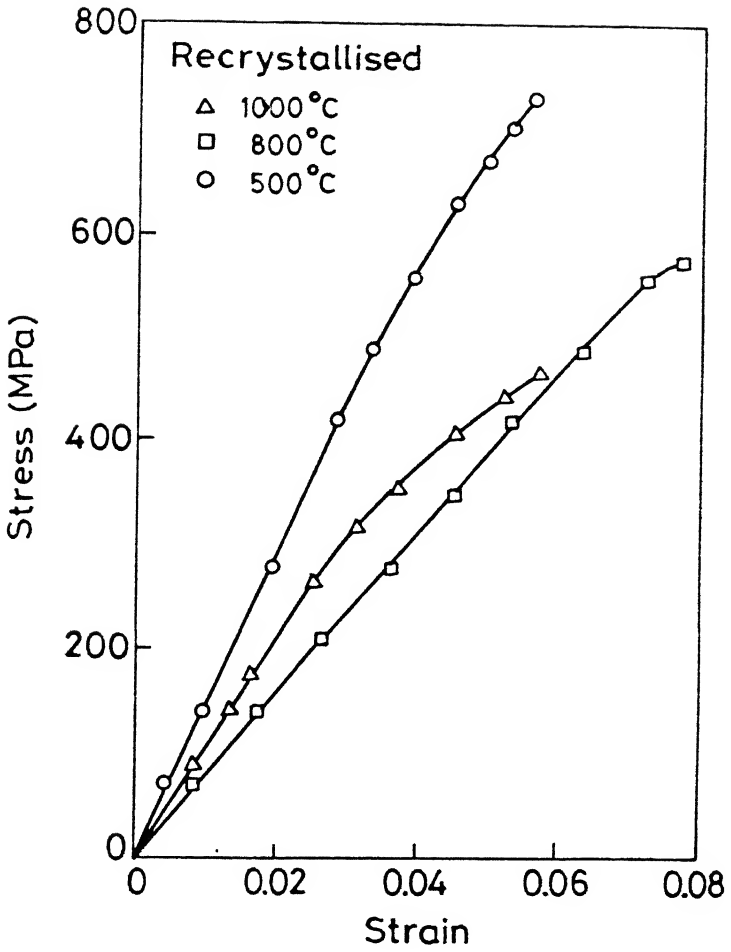

(a)

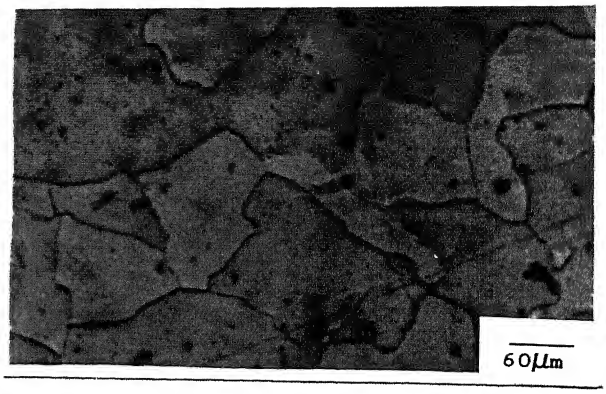

(b)

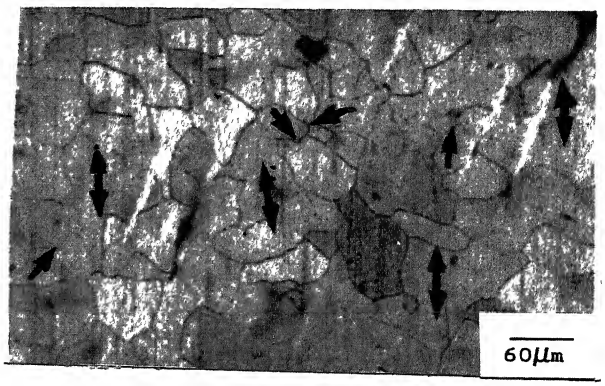

(c)

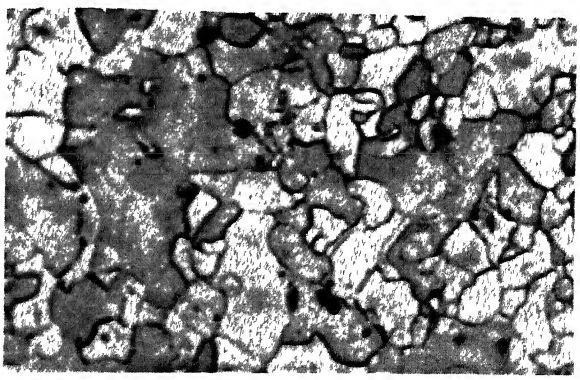

(d)

Fig.22 (a) Stress-strain behaviour of rolled and recrystallised Fe_3Al and optical micrographs of (b) rolled at 1000°C and recrystallised, (c) rolled at 800°C and recrystallised and (d) rolled at 500°C and recrystallised Fe_3Al.

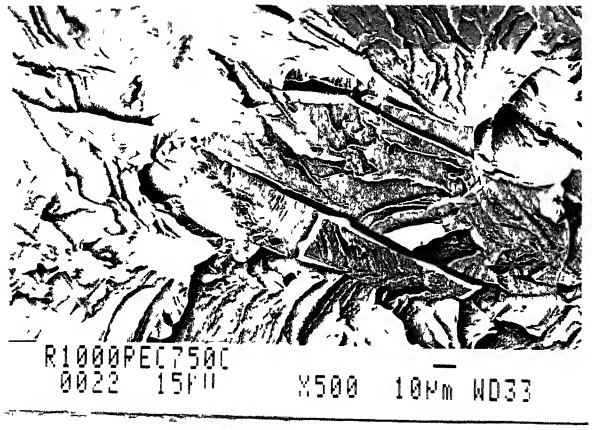

(a)

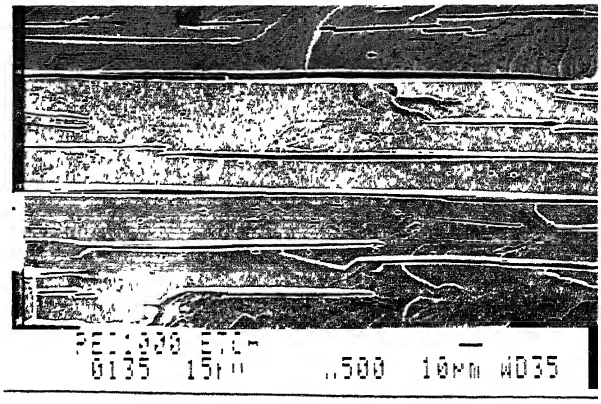

(d)

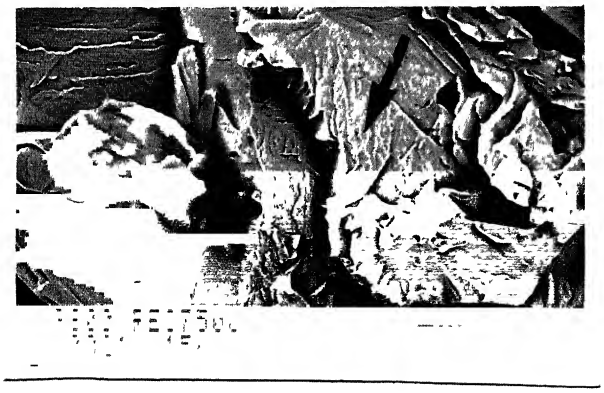

(b)

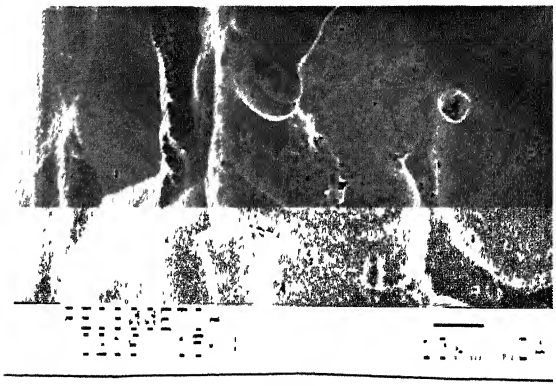

(e)

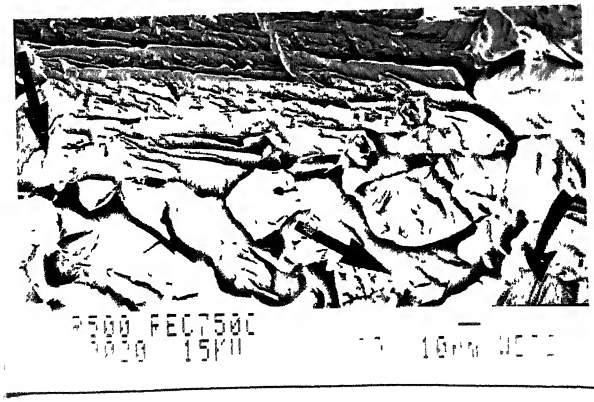

(c)

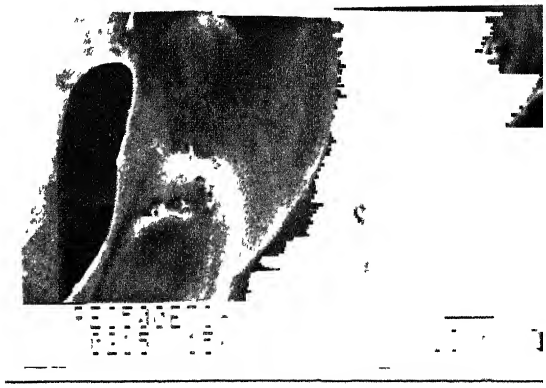

(f)

Fig.23 Fracture morphology of rolled and recrystallised iron aluminide (a) 1000°C unetched, (b) 800°C unetched, (c) 500°C unetched, (d) 1000°C etched, (e) 800°C etched and (f) 500°C etched.

size after recrystallisation [Figure 22(b),(c)and (d)]. Figure 22 (b) shows the optical microstructure of the intermetallic rolled at 1000°C and then recrystallised. This intermetallic exhibits large grain size and this resulted in lowest fracture strength. This intermetallic had undergone dynamic recrystallisation while rolling at 1000°C, which would have caused nucleation of subgrains. During annealing treatment, these subgrains would have grown and lead to nucleation and growth of equiaxed grains. Figure 22(c) shows the optical microstructure of the intermetallic rolled at 800°C. It exhibits a mixture of large subgrains (marked by↕) and equiaxed nucleated grains (marked by ↑). Equiaxed grains have nucleated as a consequence of dynamic recovery and sub-grain growth. However, these equiaxed grains have not undergone growth as in the case of the intermetallic rolled at 1000°C. Figure 22(d) shows the optical microstructure of the intermetallic rolled at 500°C and then recrystallised. Dynamic recrystallisation was negligible at the rolling temperature of 500°C (refer to Figure 19d). During annealing of this intermetallic at 750°C, small subgrains have nucleated and have grown. These grains have not grown as in the case of intermetallic rolled at 1000°C and 800°C. This intermetallic exhibits equiaxed recrystallised grains as a consequence of large amount of strain energy stored in the material after the rolling treatment. This high stored strain energy is due to the 80% severe mechanical deformation imparted to the specimen at a low rolling temperature of 500°C. This stored energy acts as a driving force for recrystallisation and thus fine equiaxed recrystallised grains were obtained. Figure 22 (d) shows

a mixture of subgrains which have exhibited growth (marked by X) and recrystallised fine equiaxed grains. Thus, material rolled at 500°C and then recrystallised exhibits highest fracture strength due to its fine grain size.

Figure 22(a) shows that the highest ductility was obtained in the case of intermetallic rolled at 1000°C and then recrystallised. This could possibly be attributed to the low grain boundary area in this material [Figure 22(b)]. Earlier McKamey and Pierce have suggested that reduction in grain boundary area leads to increase in ductility as it suppresses hydrogen diffusion into the lattice [18].

Chromium and titanium were alloyed with iron aluminides on the basis of alloy development philosophy suggested by Balasubramaniam [14]. The rolled Fe_3Al-5Cr and Fe_3Al-5Ti strips were recrystallised at 750°C for 1 hour. Table 10 presents the results of tensile testing of these alloyed iron aluminides.

The tensile stress strain curves of Fe_3Al-5Cr and Fe_3Al-5Ti are presented in Figure 24 and Figure 25,respectively. The Fe_3Al-5Ti intermetallic also exhibited a higher UTS value than Fe_3Al-5Cr intermetallic. Fracture morphology of these intermetallics has been shown in Figure 26(a)and 26(b). Fe_3Al-5Cr exhibited transgranular cleavage kind of fracture surface whereas Fe_3Al-5Ti showed a mixed mode of fracture (transgranular + intergranular). Intergranular boundaries have been marked by arrow. River like pattern can be seen with in each grain. It can be concluded from this fracture morphology that Ti additions possibly enhances cleavage strength, resulting in mixed mode

Table 10 Room temperature tensile properties of Fe_3Al-5Cr and Fe_3Al-5Ti intermetallics.

Sample	Condition	Y.S. (MPa)	UTS (MPa)	Ductility (%)	Fracture Type
Fe_3Al+Cr	R000+Rec	160	310	4.9	TG
Fe_3Al+Ti	R1000+Rec	114	629	6.8	IG+TG

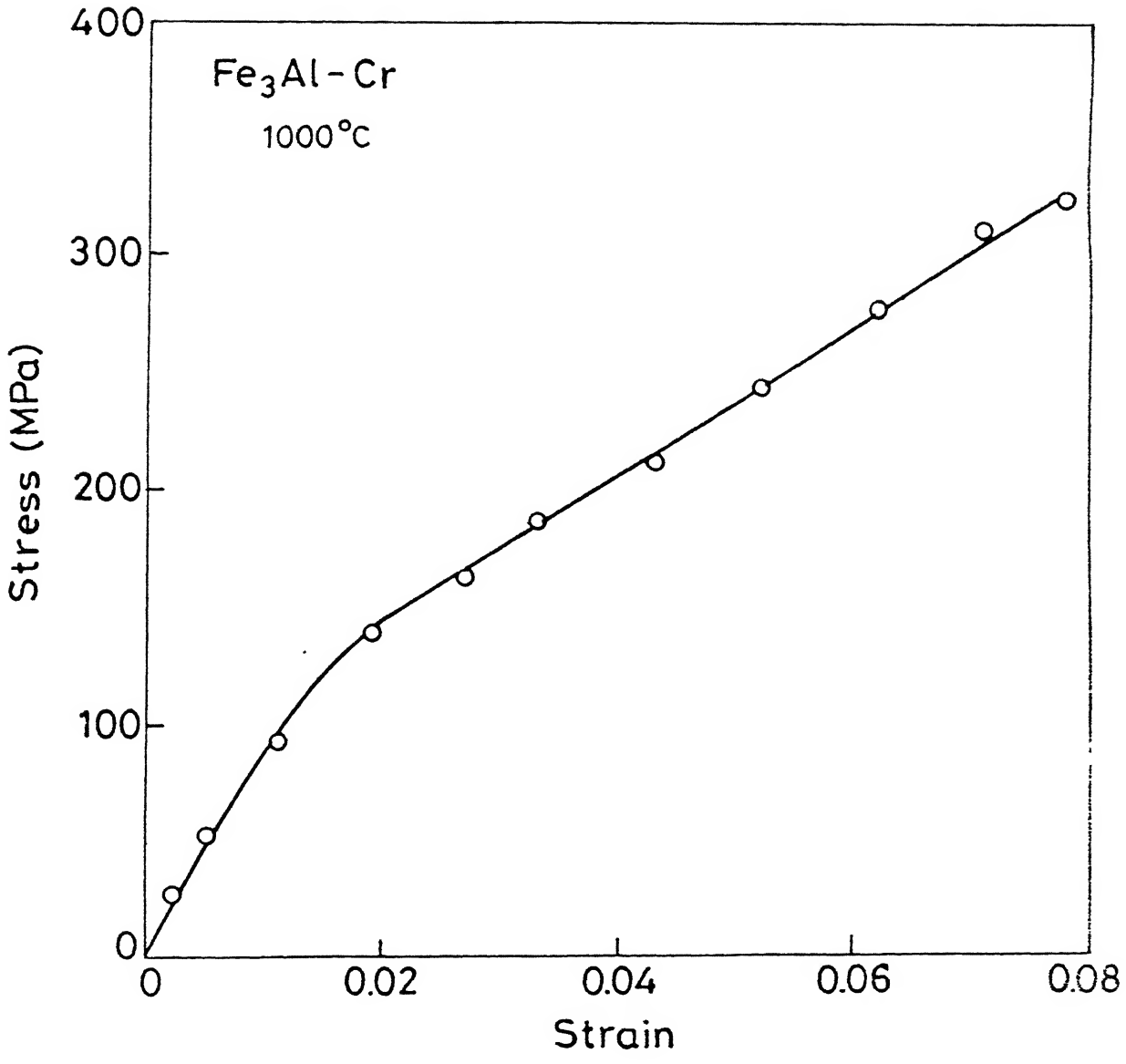

Fig.24 Stress-strain behaviour of Fe_3Al-5Cr intermetallic in air at room temperature.

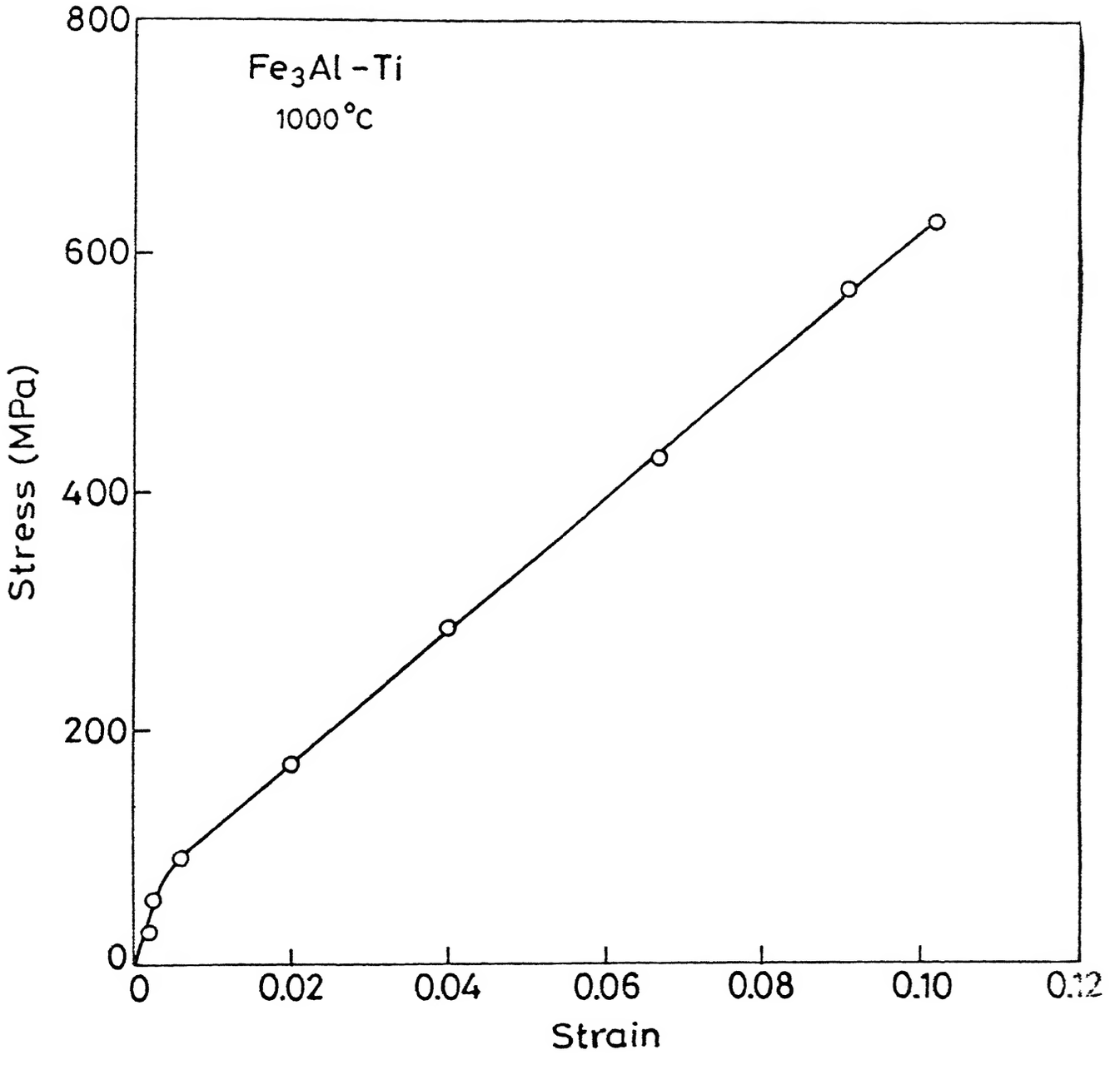

Fig.25 Stress-strain behaviour of Fe_3Al-5Ti intermetallic in air at room temperature.

(a)

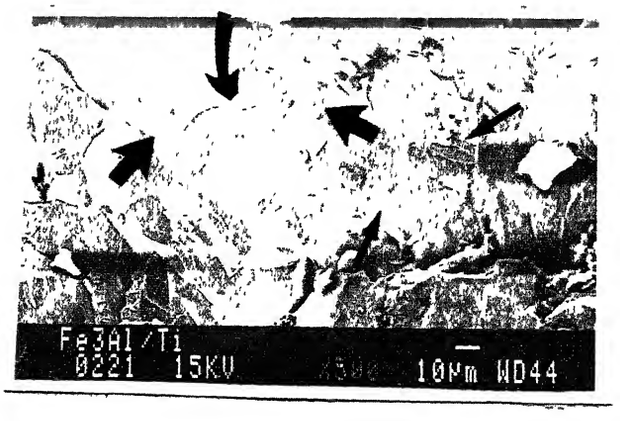

(b)

Fig.26 Fracture morphology of (a) Fe_3Al-5Cr and (b) Fe_3Al-5Ti after rolling and recrystallisation (in unetched condition).

fracture.

The sharp rise in ductility could be attributed to alloy development philosophy suggested by Balasubramanium [14]. It has been established that passivity can be induced in iron aluminides by addition of Cr and Ti. Akhtar has confirmed that Cr and addition to Fe_3Al shifts the anodic curve into passive range [36]. Corrosion rate decreased significantly with addition of passivity inducing elements (Figure 27). This implied that hydrogen liberation rate has also decreased and therefore, a lower amount of nascent hydrogen is available to the intermetallic to cause embrittlement. Thus, a higher ductility was exhibited by these alloyed iron aluminides.

Another possible reason for this increase in ductility could be attributed to the microstructure of these recrystallised intermetallics. Figure 28(a) and 28(b) show the optical micrograph of Fe_3Al-5Cr and Fe_3Al-5Ti, respectively. Mckamey et al. had earlier concluded that recrystallisation process in iron aluminides vary greatly with several variables such as alloying additions and fabrication technique [18]. Figure 28(b) exhibits partially recrystallised microstructure of Fe_3Al-5Ti (new grains marked with arrow). Earlier, it had been proved that partially recrystallised microstructure minimizes HE and improved ductility was obtained [18]. However, Fe_3Al-5Cr shows coarse grains suggesting grain growth after recrystallisation process [Figure 27(a)]. Thus, higher ductility in chromium alloyed iron aluminide could not be solely attributed to the phenomenon of partially recrystallised microstructure. This further supports that the

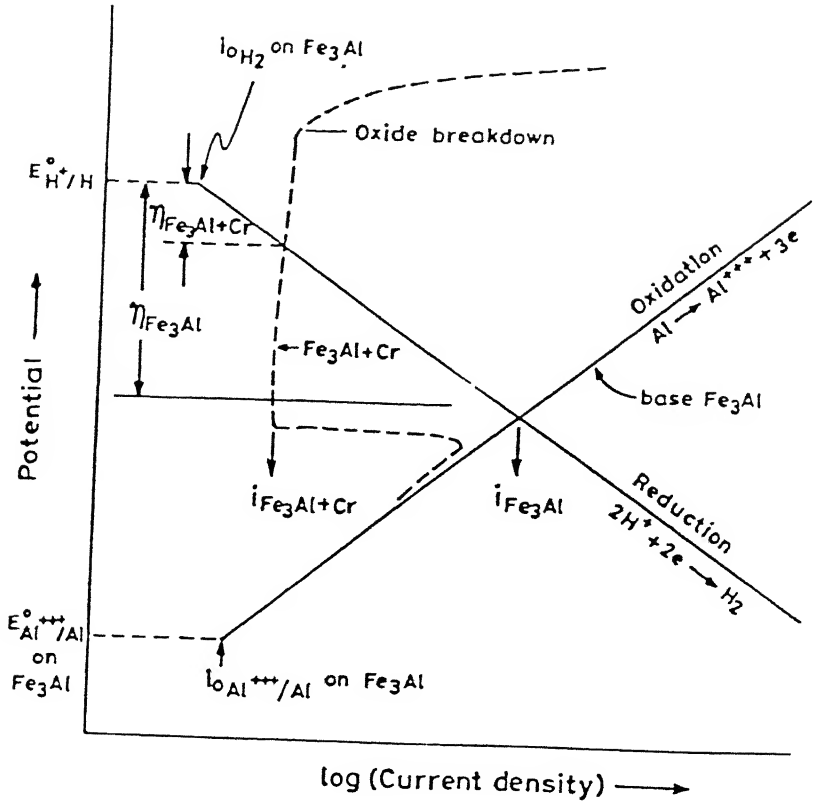

(a)

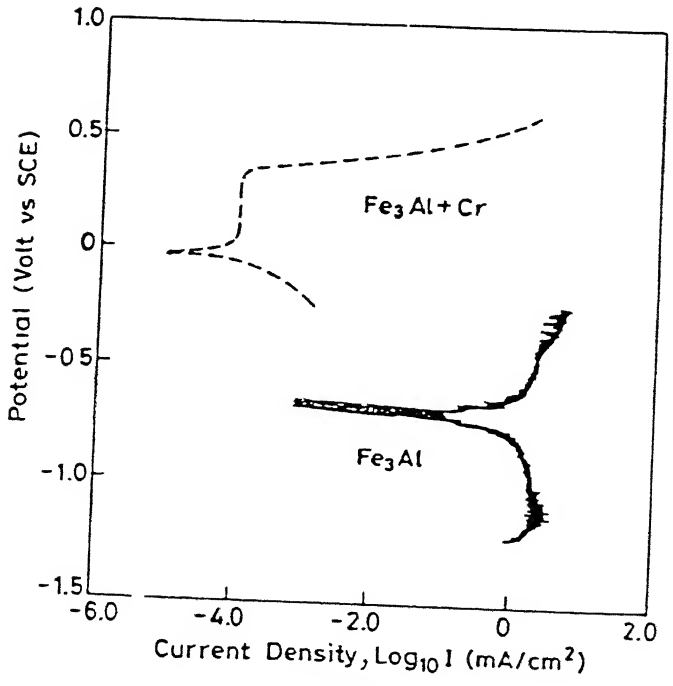

(b)

Fig.27 (a) Schematic Evan's diagram for corrosion of Fe_3Al and Fe_3Al + Cr intermetallic.

(b) Potentiodynamic polarisation curve of Fe_3Al and Fe_3Al + Cr in pH=4 H_2SO_4 solution containing 200 ppm Cl^-.

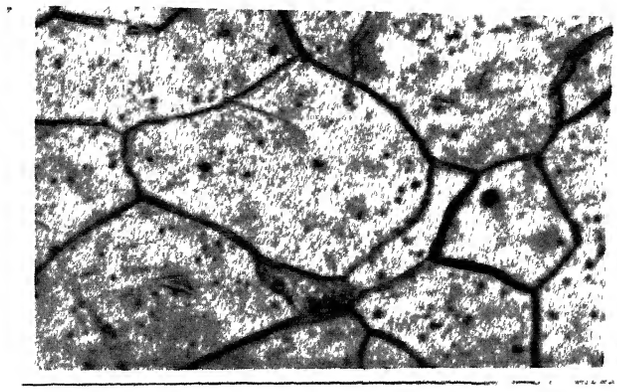

(a)

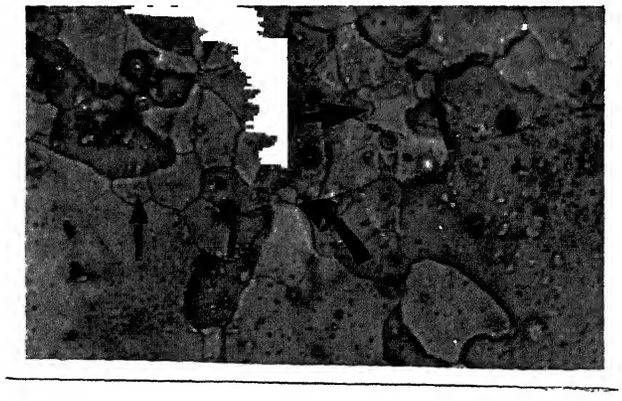

(b)

Fig.28 Optical micrographs of (a) Fe_3Al-5Cr and (b) Fe_3Al-5Ti after 80% deformation at 1000°C and recrystallised at 750°C for 1 hour.

surface passivation phenomenon in iron aluminides is responsible for improved ductility, as has also been verified by comparable ductility obtained in Cr containing and Cr free Fe_3Al in hydrogen free environments [17].

These alloyed iron aluminides exhibited low yield strength. McKamey and Liu have suggested that yield strength decreases due to solid solution softening on alloying with chromium[17]. However, low yields strength of Fe_3Al-5Ti and Fe_3Al-5Cr intermetallic is poorly understood as some other investigators have mentioned that Cr and Ti should lead to solid solution strengthening [37].

4.2.3 Rolled and Ordered Intermetallic :

The mechanical properties of rolled iron aluminides after ordering treatment of 100 hours at 500°C are presented in Table 9. Intermetallic rolled at 1000°C showed the highest fracture strength of 560 MPa while intermetallic rolled at 800°C and 500°C showed fracture strengths of 455 MPa and 360 MPa, respectively (Figure 29a). Ductility was practically zero in all the three cases. The fracture morphology in unetched condition has been shown in Figure 30(a), 30(b) and 30(c). Transgranular cleavage type of brittle fracture surfaces were observed in all these ordered intermetallics. Fracture morphology was very similar to that observed in the rolled and rolled + recrystallised intermetallic Figure 30(d), 30(e) and 30(f) shows fracture surfaces of ordered material in the etched condition. Some of the etch pits observed in Figure 30(f) were very small and their shape and size could not be resolved. Such features are indicative of

those dislocations which have not reached the crystal surface [33]. It was very difficult to resolve overlapping dislocations when dislocation density was high [Figure 30(f)]. Figure 30(e) also exhibits slip bands (marked by arrow).

Figure 29(b), 29(c) and 29(d) are the optical micrographs of material rolled at three different temperatures and then ordered. This variation in grain size contributes to the change in fracture strength of rolled and ordered intermetallic. The intermetallic rolled at 500^{o}C has the highest stored strain energy after deformation processing . This stored strain energy could have provided a greater driving force for ordering. Therefore, grain growth had occurred to greater extent in this intermetallic after heat treating at 500^{o}C for 100 hours. Thus, intermetallic rolled at 500^{o}C and then ordered for a long period revealed coarsest grain size. This coarse grain size could be the reason for its low fracture strength. The amount of stored strain energy in intermetallics rolled at 800^{o}C and 1000^{o}C would have been lower because the deformation was carried out at higher temperatures where dynamic recovery processes operate. When these intermetallics were later ordered, the new grains would have nucleated later than the intermetallic rolled at 500^{o}C and consequently, grain growth would not have occurred to the extent it had occurred in the intermetallic rolled at 500^{o}C. Along similar lines it can be argued that the intermetallic rolled at 1000^{o}C and ordered should exhibit the smallest grain size and this is reflected in Figure 29 (b).

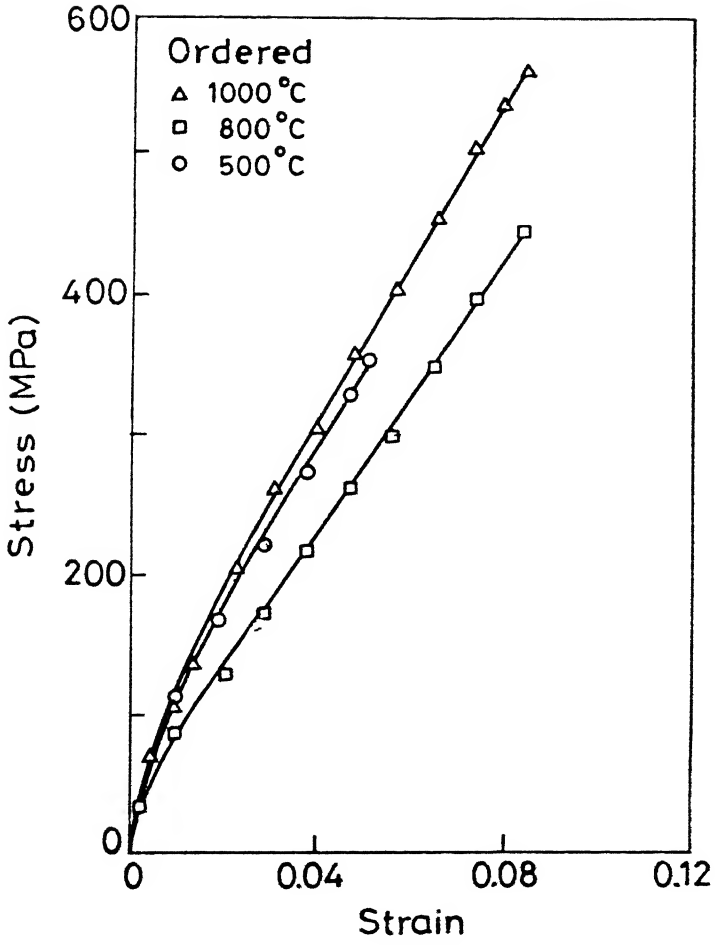

(a)

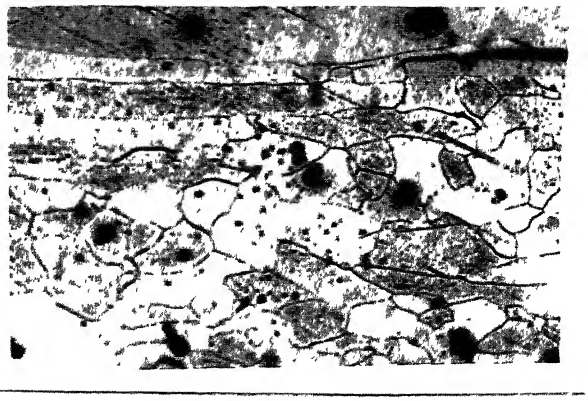

(b)

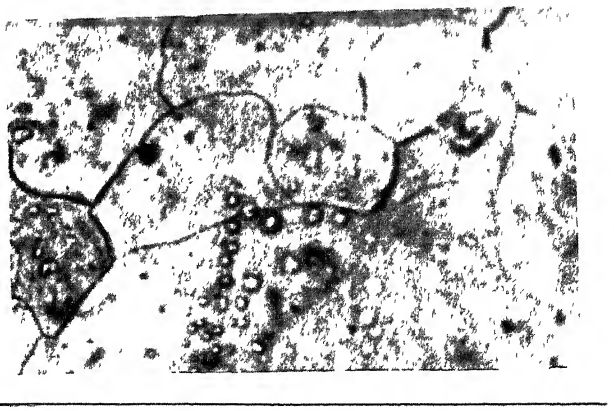

(c)

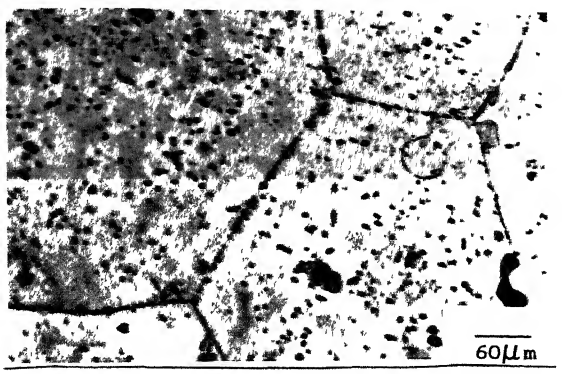

(d)

Fig.29 (a) Stress-strain behaviour of rolled and ordered Fe_3A and optical micrographs of (b) rolled at 1000°C an ordered, (c) rolled at 800°C and ordered and (d) rolle at 500°C and ordered.

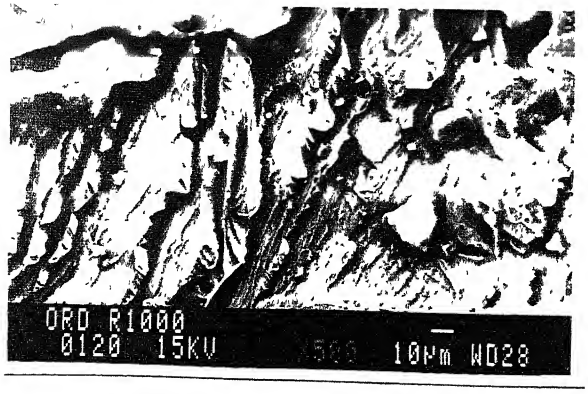

(a)

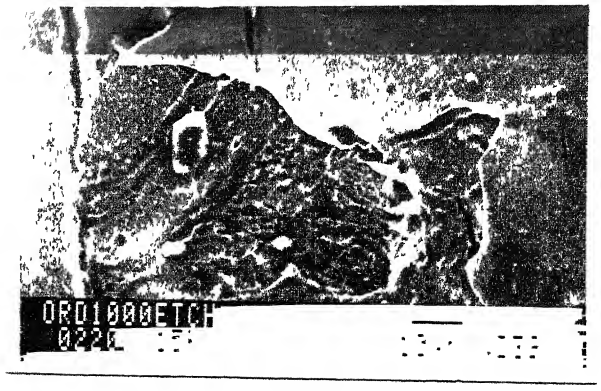

(d)

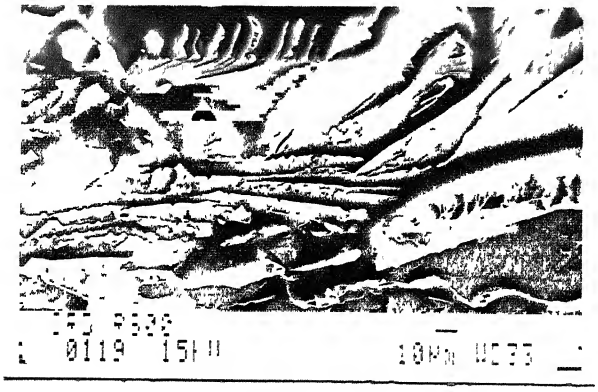

(b)

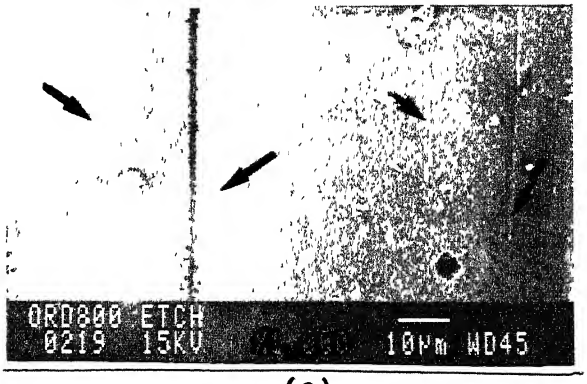

(e)

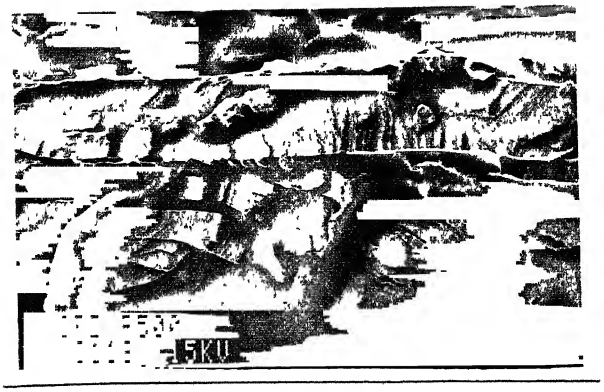

(c)

(f)

Fig.30 Fracature morphology of rolled and ordered Fe_3Al (a) 1000°C unetched, (b) 800°C unetched, (c) 500°C unetched, (d) 1000°C etched, (e) 800°C etched and (f) 500°C etched.

CHAPTER 5

CONCLUSIONS

5.1 CONCLUSIONS

The room temperature mechanical behaviour of iron aluminides were studied after a series of thermomechanical and heat treatments. The following were the salient conclusions of this study.

1. The rolled intermetallic showed highest hardness value as compared to intermetallic after recrystallisation and ordering treatments. This has been explained by cooling rate effects and nucleation of subgrains made up of <100> dislocations.
2. The presence of DO_3 phase in iron aluminide after ordering treatment has been confirmed by (440) peak broadening in the XRD pattern.
3. The intermetallic rolled at 1000°C showed greater fracture strength in the rolled condition compared to the intermetallics rolled at 800°C and 500°C because of its finer grain size. This has been explained by considering dynamic recrystallisation occurring at these temperatures and the resulting microstructures.
4. The intermetallic rolled at 500°C and then recrystallised at 750°C for 1 hour showed the highest fracture strength compared to intermetallics rolled at 800°C and 1000°C and subsequently recrystallised. However, intermetallic rolled at 1000°C and then recrystallised at 750°C for 1 hour

exhibited highest ductility. This behaviour has been ascribed to the degree of recrystallisation and the microstructure. Partially recrystallised microstructure prevents hydrogen ingress through grain boundaries and thus minimises hydrogen embrittlement.

5. The intermetallic rolled at 1000°C and then ordered at 500°C for 100 hours showed highest fracture strength compared to intermetallic rolled at 800°C and 500°C and subsequently ordered. This behaviour is due to its smaller grain size. The variation in grain size has been attributed to rapid grain growth occurring in the intermetallic rolled at lower temperature due to its higher stored strain energy.

6. Fracture morphologies were brittle and exhibited cleavage type failure in all the cases. The fractographs also revealed river flow pattern characteristic of cleavage type of fracture.

7. Etch pit study indicated that the cleavage plane/facets to be of cube orientation, e.g, of (100) type. The possible reason for this observation has been outlined based on dislocation interactions and decohesion mechanism of HE.

8. Fe_3Al-5Cr and Fe_3Al-5Ti intermetallics could be given 80% deformation successfully without cracking. Fe_3Al-5Ta could be rolled to 50% deformation while Fe_3Al-5Nb could be rolled to 40% deformation prior to cracking. Fe_3Al-5Si, Fe_3Al-5Mo and Fe_3Al-5V cracked in the first rolling pass itself. This could be due to formation of various other brittle intermetallics in ternary iron aluminides, although formation

of additional phases such as Fe_5Ta_3 and Al_3Ta_2 was confirmed only in the case of Fe_3Al-Ta intermetallic by XRD.

9. Fe_3Al-5Cr and Fe_3Al-5Ti intermetallics showed relatively high ductility values. This could possibly be due to enhancement of passivity on the surface. However, Fe_3Al-5Cr and Fe_3Al-5Ti intermetallics exhibited low yield strengths. This has been attributed to solid solution softening but this is poorly understood.

5.2 SCOPE FOR FURTHER STUDY

There are several new aspects about mechanical behaviour of iron aluminides after TMTs and heat treatments which have risen up after this study. Investigations on these aspect would provide a better understanding of development of ductile iron aluminides.

1. Transmission electron microscopy could be performed to understand the role of microstructure (after the various TMTs and heat treatments) on the dislocation interaction and also to identify the various phases in alloyed iron aluminides.
2. Fe_3Al-M type alloys could be thoroughly characterised to determine the possible reasons for cracking during deformation processing.
3. Fe_3Al-M type alloys should be prepared with lower amounts of elemental additions. The effect of composition and subsequent processing on properties could be studied.
4. All these studies of Fe_3Al and Fe_3Al-M could be coupled with detailed low temperature aqueous corrosion and high temperature oxidation studies to elucidate the nature of passive layers forming in the iron aluminides.

REFERENCES

1. N.S.Stoloff, "Orderedalloys- physical metallurgyand structural applications", Int. Metal Review. 29, 123-135 (1984).
2. C.T.Liu, J.O.Stiegler and F.H.Froes, "Ordered Intermetallics", Metals Handbook 10^{th} ed. Vol.2,(ASM Materials Park,USA) 913-942 (1990).
3. C.T.Liu and K.S.Kumar, "Ordered intermetallic alloys, Part1:Nickel and Iron Aluminides", J. Metals. 45, 38-44 (1993).
4. C.G.McKamey, J.H.Devan, P.F.Tortorelli and V.K.Sikka,"Areview of recent development in Fe_3Al based alloy", J. Mater. Res. 6, 1779-1786 (1991).
5. J.H.Devan, "Resistance of iron - aluminium alloys to oxidation at high temperatures", Oxidation of High Temperature Intermetallics; Eds. T.Grobstein and J.Doychak , TMS, Warrandale, USA, 107-115 (1989).
6. C.Sykes and J.Bampyfylde, "The physical properties of iron - aluminium alloys", J. Iron Steel Inst. 130, 389-394 (1932)
7. C.T.Liu, E.H.Lee and C.G.McKamey,"An environmental effect asthe major cause for room temperature embrittlement in FeAl", Scripta Metall. 23, 875-880 (1989).
8. A.Shan and D.Lin, "Effects of strain rate and chromium addition on room temperature ductility and fracture mode in Fe_3Al", Scripta Meatll. Mater. 27, 95-100 (1992).
9. D.B.Kasul and L.A.Heldt, "Embrittlement of B2 iron aluminide by water vapor and by hydrogen", Met.Trans. 25A, 1285-1290 (1994).

10. C.T.Liu, C.G.McKamey and E.H.Lee, "Environmental effects on room temperature ductility and fracture mode in Fe_3Al", Scripta Metall. Mater. 24, 385-390 (1990).

11. D.B.Kasul and L.A.Heldt, "Effect of environment on the mechanical properties of an Fe-24.6Al alloy", Scripta Metall. Mater. 25, 1047-1051 (1991).

12. H.K.Birnbaum, G.M.Bond and I.M.Robertson, "Effect of hydrogen on deformation and fracture processes in high purity aluminium", Acta Metall. 36, 2193-2198 (1988).

13. G.M.Bond, I.M.Robertson and H.K.Birnbaum, "On the mechanisms of hydrogen embrittlement of Ni_3Al alloys", Acta Metall.37, 1407-1411 (1989).

14. R.Balasubramniam,"Alloy development philosophy to minimize room temperature hydrogen embrittlement in iron aluminides", Scripta Metall. Mater. communicated (1994).

15. N.S. Stoloff and D.J.Duquette, "Moisture and hydrogen induced embrittlement of iron aluminides", J. Metals.45, 30-35 (1993).

16. C.G.McKamey, J.A.Horton and C.T.Liu, "Effect of chromium on room temperature ductility and fracture mode in Fe_3Al", Scripta Metall. 22, 1679-1681 (1988).

17. C.G.McKamey, and C.T.Liu," Chromium addition and environmental embrittlement in Fe_3Al", Scripta Metall. Mater. 24, 2119-2122 (1990).

18. C.G.McKamey and D.H.Pierce,"Effect of recrystallisation on room temperature tensile properties an Fe_3Al based alloy", Scripta Metall. Mater. 28, 1173-1176 (1993).

19. M.A.Crimp and K.M.Vedula,"Effect of boron on the tensile properties of B2 FeAl", Mat. Sci. Eng. 78, 193-199 (1986).

20. C.T.Liu and E.P.George, "Environmental embrittlement in boron free and boron doped FeAl alloys", Scripta Metall. Mater. 24, 1285-1290 (1990).

21. C.G McKamey and J.A.Horton,"Effect of alloying additions in ordering of iron aluminides", Met. Trans. 20A, 751-756 (1989).

22. D Lin, A.Shan and D.Li, "Superplasticity in Fe_3Al-Ti alloy with large grains", Scripta Metall. Mater. 31, 1455-1460 (1994).

23. R.G.Bordeau, "Development of iron aluminides", East Hartford CT: United Technologies Corporation, AFWAL-TR-87-4009, Eds. Pratt and Whitney (1987).

24. S.A.David, J.A.Horton, C.G.Mckamey, T.Zacharia and R.W.Reed, "Welding of iron aluminides", Weld. J. 68, 372s-381s (1989).

25. N.D.Tomashov and G.P.Chernova, "Passivity and protection of metals against corrosion", Plenum Press, New York, 66-91 (1967).

26. B.H.Rabin and R.N.Wright, "Microstructure and tensile properties of Fe_3Al produced by combustion synthesis/ hot isotactic pressing", Met. Trans. 23A, 35-40 (1992).

27 V.K.Sikka, S,Vishwanathan and C.G.McKamey, "Development and commercialization status of Fe_3Al-based intermetallic alloys", Structural Intermetallics, Eds. R.Darolia, J.J.Kewandoski, C.T.Liu, P.L.Martin and M.B.Nathal, 483-491 (1993).

28. I.Baker and Nagpal, "A review of flow and fracture of FeAl",Structural Intermetallics, Eds. R.Darolia, J.J.Kewandoski, C.T.Liu, P.L.Martin and M.B.Nathal, 463-473 (1993).

29. K.Oki, M.Hasaka and T.Eguchi, "Process of order-disorder transformation in iron-aluminium alloys", Japanese J.of Appl. Phys. 12, 1522-1530 (1973).

30. K.Oki, M.Hasaka and T.Eguchi," An XRD study of kinetic behavior of ordering in Fe_3Al alloy", Trans. Japan Inst. Metals 14, 8-13 (1973).

31. D.G.Morris and M.Leboeuf, "The role of controlled recrystallisation treatment on ductility of Fe_3Al alloys", Acta. Metall. Mater. 42, 1817-1823 (1994).

32. J.Friedel, "Dislocations", Pergamon Press, New York, 320-347 (1964).

33 J.Friedel, "Dislocations", Pergamon Press, New York, 12-21 (1964).

34. J.Friedel, "Dislocations", Pergamon Press, New York, 158-165 (1964).

35. M.V.Akdeniz, A.O.Mekhrabov and T.Yilmaj, "THe role of Si addition on the interfacial interaction in Fe-Al diffusion layer", Scripta Metall. Mater. 31, 1723-1728 (1994).

36. M.J.Akhtar, M.Tech Thesis, IIT Kanpur, India (1995).

37. D.G.Morris, M.Dadras and M.A.Morris, "The influence of chromium additions on order and ductility in Fe_3Al intermetallic", J. de Physique IV , Colloque C7, 3, 429-434 (1993).
